Influence of isoprene chemical mechanism on modelled changes in tropospheric ozone due to climate and land use over the 21st century

O. J. Squire[1], A. T. Archibald[1,2], P. T. Griffiths[1], M. E. Jenkin[3], D. Smith[1], and J. A. Pyle[1,2]

[1]Centre for Atmospheric Science, Department of Chemistry, University of Cambridge, Cambridge, CB2 1EW, UK
[2]National Centre for Atmospheric Science, Department of Chemistry, University of Cambridge, Cambridge, CB2 1EW, UK
[3]Atmospheric Chemistry Services, Okehampton, Devon EX20 1FB, UK

Correspondence to: O. J. Squire (ojsquire@gmail.com)

Abstract. Isoprene is a precursor to tropospheric ozone, a key pollutant and greenhouse gas. Anthropogenic activity over the coming century is likely to cause large changes in atmospheric CO_2 levels, climate and land use, all of which will alter the global vegetation distribution leading to changes in isoprene emissions. Previous studies have used global chemistry–climate models to assess how possible changes in climate and land use could affect isoprene emissions and hence tropospheric ozone. The chemistry of isoprene oxidation, which can alter the concentration of ozone, is highly complex, therefore it must be parameterised in these models. In this work, we compare the effect of four different reduced isoprene chemical mechanisms, all currently used in Earth system models, on tropospheric ozone. Using a box model we compare ozone in these reduced schemes to that in a more explicit scheme (the Master Chemical Mechanism) over a range of NO_x and isoprene emissions, through the use of O_3 isopleths. We find that there is some variability, especially at high isoprene emissions, caused by differences in isoprene-derived NO_x reservoir species. A global model is then used to examine how the different reduced schemes respond to potential future changes in climate, isoprene emissions, anthropogenic emissions and land use change. We find that, particularly in isoprene-rich regions, the response of the schemes varies considerably. The wide-ranging response is due to differences in the model descriptions of the peroxy radical chemistry, particularly their relative rates of reaction towards NO, leading to ozone formation, or HO_2, leading to termination. Also important is the yield of isoprene nitrates and peroxyacyl nitrate precursors from isoprene oxidation. Those schemes that produce less of these NO_x reservoir

species, tend to produce more ozone locally and less away from the source region. We also note changes in other key oxidants such as NO_3 and OH (due to the inclusion of additional isoprene-derived HO_x recycling pathways). These have implications for secondary organic aerosol formation, as does the inclusion of an epoxide formation pathway in one of the mechanisms. By combining the emissions and O_3 data from all of the global model integrations, we are able to construct isopleth plots comparable to those from the box model analysis. We find that the global and box model isopleths show good qualitative agreement, suggesting that comparing chemical mechanisms with a box model in this framework is a useful tool for assessing mechanistic performance in complex global models. We conclude that as the choice of reduced isoprene mechanism may alter both the magnitude and sign of the ozone response, how isoprene chemistry is parameterised in perturbation experiments such as these is a crucially important consideration. More measurements and laboratory studies are needed to validate these reduced mechanisms especially under high-volatile-organic-compound, low-NO_x conditions.

1 Introduction

The emission of volatile organic compounds (VOCs) into the atmosphere in the presence of NO_x (the sum of nitric oxide (NO) and nitrogen dioxide (NO_2)) can lead to the formation of tropospheric ozone (O_3), which is a pollutant and greenhouse gas (e.g. Haagen-Smit, 1952). One VOC that contributes significantly to tropospheric O_3 production

is the biogenically emitted di-alkene isoprene (2-methyl-1,3-butadiene) with annual emissions of $\sim 500\,\text{Tg C}$ (Guenther et al., 2006). Isoprene is highly reactive with an atmospheric lifetime on the order of about 1–2 h, and thus has the potential to strongly influence levels of tropospheric O_3 both regionally (e.g. Chameides et al., 1988) and globally (e.g. Wang and Shallcross, 2000).

Isoprene is oxidised in the atmosphere by the hydroxyl radical (OH), O_3 and the nitrate radical (NO_3). These reactions initiate a complex cascade of photochemical interactions, which (theoretically) comprise $> 10^5$ reactions involving $> 10^4$ species (Aumont et al., 2005). Including all of these reactions in 3-D global modelling studies is too computationally expensive and so isoprene chemistry must be parameterised. Furthermore, our understanding of isoprene oxidation is incomplete; only a small number of these 10^5 reactions are known in depth. Although parameterisation is a necessity, it introduces uncertainties in the chemistry and subsequent calculation of trace gas composition, as multiple species or reactions have to be lumped together. Furthermore, there are several different methodologies for how best to parameterise an explicit chemical mechanism, which has led to the existence of a plethora of different reduced schemes, whose use in models can lead to different results (e.g. Archibald et al., 2010b). Jeffries et al. (1992) laid out a set of basic considerations to make when evaluating a condensed chemical mechanism, which are the points in the process of condensed mechanism development where individual methodologies may diverge. These include the relationship between different lumping groups and explicit species, the method used to select individual lumping groups, e.g. by characteristic reaction times, molecular weight or chemical structure, and the approach to handling chain degradation kinetics for each lumped species. The choices made in developing reduced mechanisms may also have been made with the aim of accurately representing specific timescales (e.g. urban or continental) or species (e.g. O_3) (Jeffries et al., 1992).

To date there have been several studies that calculate the effects of future isoprene emission changes caused by potential climate and land use scenarios on surface O_3 (Sanderson et al., 2003; Wiedinmyer et al., 2006; Ganzeveld et al., 2010; Wu et al., 2012; Pacifico et al., 2012), including our recent study (Squire et al., 2014). These 3-D global modelling studies all use (often different) reduced isoprene mechanisms. Very few studies, however, have attempted to quantify the influence of differences in the isoprene scheme on the O_3 response. Previously, von Kuhlmann et al. (2004) compared three different isoprene mechanisms and related parameters such as the deposition of intermediates, the treatment of isoprene nitrates and the emission strength of O_3 precursors, all within a particular global model. Here we explore the behaviour of four reduced schemes, all designed to be used in complex Earth system models (ESMs), in the context of the climate and land use perturbation experiments carried out in Squire et al. (2014). Given the importance of O_3 in the

Earth system (Huntingford et al., 2011), our analysis focuses specifically on O_3 and on O_3 precursors.

Even without mechanism reduction, there exist sources of uncertainty in isoprene oxidation that are associated with our fundamental lack of understanding about certain aspects of the chemistry. One such aspect is the degree to which HO_x is regenerated from isoprene degradation under low-NO_x high-VOC conditions. Several campaigns in such conditions (GABRIEL, Kubistin et al., 2010; INTEX-A, Ren et al., 2008; OP3, Stone et al., 2011; Whalley et al., 2011) reported levels of HO_x that were higher than expected, considering the high reactivity of isoprene with OH ($k_{298\,\text{K}} = 10^{-10}\,\text{cm}^3\,\text{molecule}^{-1}\,\text{s}^{-1}$). Proposals have been put forward for missing mechanistic pathways, e.g. peroxy radical isomerisation (Peeters et al., 2009), and epoxide formation (Paulot et al., 2009) which to some extent reconcile these discrepancies (Archibald et al., 2010a; Warwick et al., 2013; Fuchs et al., 2013). It has also been demonstrated that positive biases in the measurement of HO_2 (Fuchs et al., 2011) and OH (Mao et al., 2012) cannot be ruled out in some of those field campaigns listed above. Mao et al. (2012) found that, for a Californian forest environment, taking into account these biases in addition to the proposed mechanistic pathways, gave good agreement between modelled and measured HO_x.

The chemistry of isoprene nitrates represents another important source of uncertainty. When hydroxyperoxy radicals from OH-initiated isoprene oxidation (ISO_2) react with NO, the major pathway leads to the formation of alkoxy radicals and NO_2 (leading to O_3 formation). However, there is a minor channel that leads to the formation of isoprene nitrates, which act to sequester NO_x. There are several uncertainties surrounding the chemistry of isoprene nitrates. First, estimates of the yield of isoprene nitrates from the OH / NO channel range from 4.4 to 15 % (Xie et al., 2013, and references therein). Modelling studies have shown that the assumed yield of isoprene nitrates can have a large impact on tropospheric O_3 (e.g. von Kuhlmann et al., 2004; Wu et al., 2007; Paulot et al., 2012). Second, isoprene nitrates may also be formed from the oxidation of isoprene by NO_3, which is estimated to account for 30–60 % of isoprene nitrate production (von Kuhlmann et al., 2004; Horowitz et al., 2007; Paulot et al., 2012). The types of isoprene nitrates formed via the NO_3 pathway are distinct from those formed via the OH / NO pathway and details of their atmospheric fates remain relatively obscure (Xie et al., 2013). Third, once formed, isoprene nitrates are readily photooxidised (lifetime ~ 4 h with respect to OH (OH $= 10^6\,\text{molecule cm}^{-3}$)), leading either to release of NO_x, or to second-generation nitrates, retaining the nitrate group. The degree to which NO_x is regenerated from isoprene nitrate degradation remains uncertain (Fiore et al., 2012; Xie et al., 2013) and has a significant effect on the O_3 response to isoprene emission changes (Paulot et al., 2012). Fourth, dry deposition of isoprene nitrates, which may represent an important NO_x sink

in isoprene-rich regions, is also uncertain, with measured deposition velocities ranging from $0.4\,\mathrm{cm\,s}^{-1}$ (Shepson et al., 1996) to $2.7\,\mathrm{cm\,s}^{-1}$ (Farmer and Cohen, 2008). Finally, there is evidence for the importance of O_3-initiated isoprene nitrate degradation (Lockwood et al., 2010) and fast photolysis of isoprene nitrates (Müller et al., 2014). In this study, the isoprene schemes we compare have a range of different parameterisations for isoprene nitrates.

In Sect. 2, we describe in detail the four chemical mechanisms used in this study and the methodology for the global perturbation experiments. In Sect. 3, we discuss the results of a series of box model simulations with the aim of comparing the four reduced mechanisms to the Master Chemical Mechanism (MCM). This is done for a range of NO_x and isoprene concentrations. Global integrations with each mechanism are then conducted to examine the effect of changes in climate, in isoprene emissions with climate, in anthropogenic emissions and in land use. In Sects. 4–6, we analyse the results of these global perturbation experiments.

2 Methods

In this section, we outline the experiments conducted to ascertain the effect of using different reduced isoprene chemical mechanisms in the context of global climate, emissions and land use change experiments (Sect. 2.2.2). In Sect. 2.1, details of the reactions and species that make up the reduced mechanisms are given.

2.1 Isoprene chemical mechanisms

The species included in each mechanism are given in Table 1, whilst a comparison of the reactions is given in Table 2. The different isoprene mechanisms were each embedded in an otherwise identical tropospheric chemistry mechanism simulating the chemistry of methane, ethane, propane, HO_x and NO_x, following O'Connor et al. (2014).

The first simulation used the UM-UKCA Chemistry of the Troposphere (CheT) mechanism, as was done for all integrations in Squire et al. (2014). The CheT isoprene mechanism consists of 16 species and 44 reactions (see Tables 1 and 2), and is based on the Mainz Isoprene Mechanism (MIM) (Pöschl et al., 2000). MIM was developed from a reduction of the Master Chemical Mechanism (version 2) (Jenkin et al., 1997), by lumping species based on their structure (e.g. all hydroxyperoxy radicals were lumped as ISO_2, and methacrolein and methyl vinyl ketone as methacrolein, MACR). The overall CheT mechanism also forms the base case against which all the schemes studied, are compared.

Since the creation of MIM, there have been a number of developments in our understanding of isoprene chemistry concerning issues such as those discussed in the Introduction. In a report compiled for the UK Met Office (Jenkin, 2012), these new developments were incorporated into the current CheT framework. The resulting updated mechanism (which will be referred to as CheT2, see Tables 1 and 2) is the most complex mechanism used in this study, consisting of 24 species and 59 reactions, and is traceable to the MCM version 3.2 (MCMv3.2).

The following is a summary of the changes introduced into the CheT mechanism to create CheT2. First, changes to the chemistry of first-generation isoprene nitrates (ISON) were made. In CheT, NO_x is regenerated from ISON by photolysis or conversion to second-generation nitrates (NALD) followed by reaction with OH. In CheT2, the overall yield of NO_x from ISON was increased, in line with recent measurements (Perring et al., 2009), by increasing the ISON photolysis rate and adding an $ISON + OH \rightarrow NO_2$ reaction channel. O_3 initiated degradation of ISON was also added based on the evidence of Lockwood et al. (2010) – it should be noted, however, that Lee et al. (2014) found that Lockwood et al. (2010) substantially overestimated the rate of this reaction. Secondly, CheT2 includes the formation of hydroperoxy-aldehydes (HPALDs) from ISO_2 and subsequent rapid release of OH (Peeters et al., 2009). This leads to more HO_x regeneration in low-NO_x high-isoprene conditions, bringing modelled and measured values closer together (e.g. Archibald et al., 2010a). The formation of isoprene epoxydiols (IEPOX) from the oxidation of isoprene hydroxy-hydroperoxides (ISOOH), a potential source of secondary organic aerosols (Paulot et al., 2009), was also included in CheT2. Finally, the yield of peroxymethacrylic nitric anhydride (MPAN) from isoprene oxidation was revised down from its CheT value (Jenkin, 2012).

The Air Quality in the Unified Model (AQUM) scheme, which was developed to deliver regional air quality forecasts and conduct air quality studies to inform emission control policies (Savage et al., 2013), was also investigated. The mechanism has a more anthropogenic VOC focus and a less detailed isoprene scheme compared with CheT (17 species, 23 reactions). Two important simplifications in the isoprene scheme are that (1) isoprene nitrates are not formed from the OH initiated pathway via the reaction of ISO_2 with NO, and (2) there is no production of MPAN.

The last and most simple isoprene scheme investigated was the super-fast chemistry scheme developed at the Lawrence Livermore National Laboratory (LLSF) (Cameron-Smith et al., 2009) for use in the Community Earth System Model (CESM – http://www.cesm.ucar.edu/models/cesm1.0/). The LLSF isoprene scheme only considers the reactions of isoprene with OH and O_3, and was parameterised based on the net effect of a more complex isoprene mechanism (Cameron-Smith et al., 2009). Aside from not including isoprene chemistry at all, it is about as simple an approximation of isoprene chemistry as is currently used in ESMs, but is still a significant improvement over neglecting isoprene chemistry altogether (Cameron-Smith et al., 2009). The scheme was developed for use in very long

Table 1. List of chemical species included in each of the isoprene mechanisms. Note that names of some of the species in AQUM were changed from the names given in Savage et al. (2013) to be consistent with the other schemes. These are as follows: "HOIPO2" – ISO_2, "MVK" – MACR, "MVKOOH" – MACROOH, "HOMVKO2" – $MACRO_2$.

Species	Description	CheT	CheT2	AQUM	LLSF
C_5H_8	isoprene	X	X	X	X
ISO_2	hydroxyperoxy radicals from $C_5H_8 + OH$	X	X	X	
ISOOH	β-hydroxyhydro-peroxides from $ISO_2 + HO_2$	X	X	X	
ISON	β-hydroxy alkylnitrates from $ISO_2 + NO$ and alkyl nitrates from $C_5H_8 + NO_3$	X	X	X	
MACR	methacrolein, methyl vinyl ketone and other C_4-carbonyls	X	X	X	
$MACRO_2$	peroxy radicals from $MACR + OH$	X	X	X	
MACROOH	hydroperoxides from $MACRO_2 + HO_2$	X	X	X	
MPAN	peroxymethacrylic nitric anhydride and other higher peroxy-acylnitrates	X	X		
HACET	hydroxyacetone and other C_3-ketones	X	X		
NALD	nitrooxy-acetaldehyde	X	X		
IEPOX	epoxydiols		X		
HPALD	hydroperoxy-aldehydes		X		
PACALD	peroxy-acid-aldehydes		X		

global 3-D integrations, where reducing computational cost is paramount.

2.2 Model experiments

2.2.1 Box model experiments

A box model comparison study was performed with the different isoprene schemes to establish any inherent differences in the schemes that do not arise from the complexity present in a global 3-D model. This also allows us to compare the reduced schemes with a more complex scheme, the MCMv3.2 (Jenkin et al., 1997; Archibald et al., 2010b), which is too complex to put into a global 3-D chemistry–climate model. The detailed nature of the MCM lends itself to being a benchmark mechanism against which the others can be compared

(e.g. Archibald et al., 2010b). However, the MCM still contains approximations; e.g. many of the rate constants are inferred from other reactions using structure reactivity relationships (SARs, e.g. Kwok and Atkinson, 1995; McGillen et al., 2011), and only four of the six ISO_2 isomers are included. Furthermore, many of the recent discoveries such as the isomerisation chemistry of ISO_2 and methacrolein are not included.

For our box model comparison, the Kinetic PreProcessor (KPP) solver (Sandu and Sander, 2006) was used, with a model time step of 20 min. The model was set up so that different emissions of NO_x and isoprene were input, allowing us to study how the mechanisms compared over a wide range of NO_x-to-isoprene ratios. NO_x emissions between 0.001 and 0.5 mg N m^{-2} h^{-1} and isoprene emissions between 0.0001 and 6 mg C m^{-2} h^{-1} were used, with emission rates

Table 2. Isoprene mechanism for CheT and differences between the CheT mechanism and the CheT2, AQUM and LLSF mechanisms. If a reaction is blank then it is exactly the same as in CheT, such that only the differences are shown. All rate constants (k) are in units of $10^{-14} cm^3$ molecule^{-1} s^{-1}. Those species not defined in Table 1 or in the main text are defined here: HCOOH – formic acid, H_2O_2 – hydrogen peroxide, HCHO – formaldehyde.

Reactants	Products			
	CheT	CheT2	AQUM	LLSF
$C_5H_8 + OH$	ISO_2			$2 MeO_2 - 1.5 OH$
k	9990		10100	
$C_5H_8 + O_3$ (1)	$1.95 MACR + 1.74 HCHO$ $+ 0.3 MACRO_2 + 0.3 MeCO_3$		$2 MACR + 1.56 CO$ $0.44 HCHO + 0.54 HO_2$	$0.87 HCHO + 1.86 MeO_2$ $+ 0.06 HO_2 + 0.05 CO$
k	0.0004		0.0006	0.0013
$C_5H_8 + O_3$ (2)	$0.24 MeO_2 + 0.84 HCOOH$ $+ 0.42 CO + 0.27 H_2O_2$		not included	not included
k	0.0004			
$C_5H_8 + O_3$ (3)	$0.75 HO_2 + 0.75 OH$		$0.54 OH$	not included
k	0.0004		0.0006	
$C_5H_8 + NO_3$	ISON	$ISON + HO_2$	$ISON + HO_2$	not included
k	69.6		67.8	
$ISO_2 + NO$ (1)	$NO_2 + MACR$ $HCHO + HO_2$		$MACR + NO_2$ $HCHO + HO_2$	not included
k	813		381	
$ISO_2 + NO$ (2)	ISON		not included	not included
k	37.5	32.6		
$ISO_2 + HO_2$	ISOOH			not included
k	89.4		103	
$ISO_2 + ISO_2$	$2 MACR + HCHO$ $+ HO_2$	$2 MACR + 2 HCHO$ $+ 2 HO_2$	not included	not included
k	200			
$ISO_2 + MeO_2$	not included	not included	$MACR + HCHO$ $+ 2 HO_2$	not included
k			50	
$ISO_2 + N_2$	not included	$MACR + HCHO$ $+ OH$	not included	not included
k		3.85×10^{10}		
$ISO_2 + O_2$	not included	$HPALD + HO_2$	not included	not included
k		2.56×10^{11}		
$MACR + h\nu$	$MeCO_3 + HCHO$ $+ CO + HO_2$		not included	not included
$MACR + OH$ (1)	$MACRO_2$			not included
k	266		1880	
$MACR + OH$ (2)	$MACRO_2$		not included	not included
k	510			
$MACR + O_3$ (1)	$1.8 MGLY + 0.9 HCOOH$ $+ 0.64 HO_2 + 0.44 CO$		$2 MGLY + 1.52 CO$ $0.48 HCHO + 0.72 HO_2$	not included
k	0.00013		0.000199	
$MACR + O_3$ (2)	$0.38 OH + 0.2 MeCO_3$		$0.72 OH$	not included
k	0.00013		0.000199	
$MACR + O_3$ (3)	$1.8 MGLY + 0.9 HCOOH$ $+ 0.64 HO_2 + 0.44 CO$		not included	not included
k	0.0000305			
$MACR + O_3$ (4)	$0.38 OH + 0.2 MeCO_3$		not included	not included
k	0.0000305			
MACR dry dep	included		not included	not included
$MACRO_2 + NO_2 + M$	MPAN $KFPAN$	KFPAN*0.107	not included	not included
$MACRO_2 + NO$ (1)	$2 NO_2 + 0.5 MeCO_3$ $+ 0.5 HACET + 0.5 CO$		$NO_2 + HO_2$ $HCHO + MGLY$	not included
k	425	452	837	
$MACRO_2 + NO$ (2)	$MGLY + 1.5 HCHO$ $+ 1.5 HO_2$		not included	not included
k	425	452		
$MACRO_2 + HO_2$	MACROOH			not included
k	1428		1479	

Table 2. Continued.

Reactants	Products			
	CheT	CheT2	AQUM	LLSF
$MACRO_2 + MACRO_2$ (1)	2 HACET + 2 MGLY + HCHO + CO		not included	not included
k	100			
$MACRO_2 + MACRO_2$ (2)	2 HO_2		not included	not included
k	100			
ISON + $h\nu$	NO_2 + MACR + HCHO + HO_2		not included	not included
k	1300	3340		
ISON + OH (1)	HACET + NALD	0.78 HACET + 0.78 NALD + 0.78 HO_2	MACR + NO_2	not included
k	1300	1940	4160	
ISON + OH (2)	not included	0.44 NO_2 + 0.44 MACR + 0.44 HCHO	not included	not included
k		0.00313		
ISON + O_3 (1)	not included	NALD + OH		
k		0.00607		
ISON + O_3 (2)	not included	MACR + HCHO NO$_2$		
k		0.00313		
ISON wet dep	included			not included
ISON dry dep	included		not included	not included
HCOOH + OH	HO_2		not included	not included
k	45			
HCOOH wet dep	included		not included	not included
HCOOH dry dep	included		not included	not included
ISOOH + $h\nu$	OH + MACR + HCHO +HO_2		OH + MACR + HCHO + HO_2	not included not included
ISOOH + OH (1)	MACR + OH			
k	10000	894		
ISOOH + OH (2)	not included	IEPOX + OH		
k		8064		
ISOOH wet dep	included		not included	not included
ISOOH dry dep	included		not included	not included
MPAN + $h\nu$			not included	not included
MPAN + M	$MACRO_2$ + NO_2		not included	not included
MPAN + OH	HACET + NO_2		not included	not included
k	2900			
MPAN dry dep	included		not included	not included
HACET + $h\nu$	$MeCO_3$ + HCHO + HO_2		not included	not included
HACET + OH	MGLY + HO_2		not included	not included
k	300	445		
HACET wet dep	included		not included	not included
HACET dry dep	included		not included	not included
MACROOH + $h\nu$ (1)	2OH + 2HO_2		OH + MGLY + HCHO + HO_2	not included
MACROOH + $h\nu$ (2)	HACET + CO + MGLY + HCHO		not included	not included
MACROOH + OH	$MACRO_2$		MGLY + HCHO + OH	not included
k	3000		5770	
MACROOH wet dep	included			not included
MACROOH dry dep	included			not included
NALD + $h\nu$	HCHO + CO		not included	not included
	NO_2 + HO_2		not included	not included

Table 2. Continued.

| Reactants | Products | | | |
	CheT	CheT2	AQUM	LLSF
$NALD + OH$	$HCHO + CO$ $+ NO_2$		not included	not included
k	1500	155		
NALD dry dep	included		not included	not included
$MACRO_2 + MeO_2$	not included		$MGLY + HCHO$ $2 HO_2$	
k			200	
$HPALD + h\nu$	not included	$PACALD + HO_2$ $+ OH$		
$HPALD + OH$	not included	$MGLY + CO$ $+ HCHO + OH$		
k		7610		
$IEPOX + OH$	not included	$MACRO_2$		
k		913		
IEPOX dry dep	not included	included		
IEPOX wet dep	not included	included		
$PACALD + h\nu$	not included	$CO + HO_2$ $+ MGLY + OH$		

being constant for the duration of a given model run. Atmospheric pressure (1×10^5 Pa) and temperature (298 K) were kept constant, and the amount of light varied through the day as in a grid cell at 14° latitude on Julian day 172 (solar declination angle = 23.44°). To ensure that differences in the oxidation chemistry were not due to differences in photolysis between the mechanisms, the MCM photolysis parameterisation was used in all cases. Details of how photolysis coefficients are calculated using this parameterisation are given in Jenkin et al. (1997). The model was initialised with 30 ppb O_3, 1820 ppb CH_4, 102 ppb CO, and run with a fixed amount of H_2O (50 %).

The box model does not include any advection or deposition processes, and, as such, O_3 values are likely to be higher than those measured in the field or calculated in UM-UKCA. Other consequences of including emissions but not removal pathways are that steady state will never be reached and long-lived reservoir species will accumulate. For example, OH could be modified by accumulation of H_2O_2 via $OH + H_2O_2$. To minimise such effects on oxidant fields, a relatively short run length of 3 days for the simulations was chosen. In all simulations, the maximum O_3 value on the third day was used to provide a consistent point of comparison between mechanisms. The results of the box model comparison are given in Sect. 3.

2.2.2 Global perturbation experiments

To investigate the influence of variations in the isoprene mechanism on potential changes in tropospheric O_3 over the 21st century, a global chemistry–climate model (the UK Met Office Unified Model coupled to the UK Chemistry and Aerosol model, UM-UKCA) was used, as specified in Squire et al. (2014). For each mechanism investigated, a present-day

(2000) integration was conducted, following the model setup described for the BASE run in Squire et al. (2014). Then, for each mechanism four future (2095) integrations were conducted to investigate (1) CC, climate change only, (2) IC, isoprene emission change with climate, (3) AC, anthropogenic emission change, and (4) LC, land use change, with each integration set up as described in Squire et al. (2014). The effect of mechanistic changes on the O_3 response to including the CO_2 inhibition of isoprene emissions was not investigated in this study. It should also be noted that with the change in land use, we assume no change in NO_x emissions.

For CC, all parameters, including isoprene emissions, remained as in the present day BASE run except sea surface temperatures, sea ice concentrations and greenhouse gas concentrations. In IC, isoprene emissions were allowed to vary with a scenario of future climate change. This led to globally higher isoprene emissions (545 Tg C yr^{-1}) than in the BASE run (467 Tg C yr^{-1}), largely due to the effect of extended CO_2 fertilisation of the biosphere under the elevated CO_2 levels. AC was characterised by stringent emission cuts across much of the Northern Hemispheric developed regions, leading to lower NO_x levels there. For LC, we used a scenario of future cropland expansion that is dominated by the replacement of tropical broadleaf trees with crops (see Squire et al. (2014) for details). As the crops emit less isoprene than broadleaf trees (Guenther et al., 2006; Lathiere et al., 2010), this causes a decrease in isoprene emissions (190 Tg C yr^{-1} globally).

3 Mechanism intercomparison with a box model

In this section we discuss the results of the simulations we performed to assess the performance of the isoprene mecha-
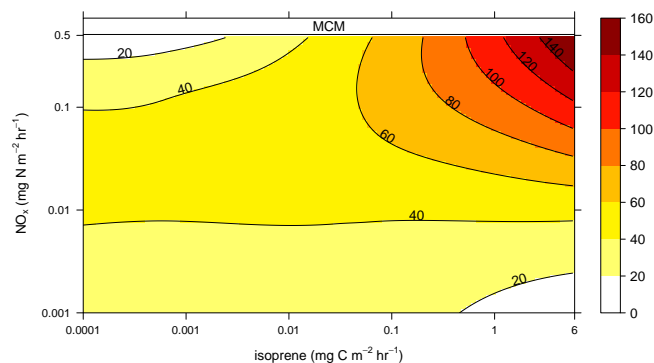
Figure 1. O_3 (ppb) isopleth plot as a function of NO_x and isoprene emissions for the Master Chemical Mechanism (MCMv3.2). This was created from a series of box model runs.
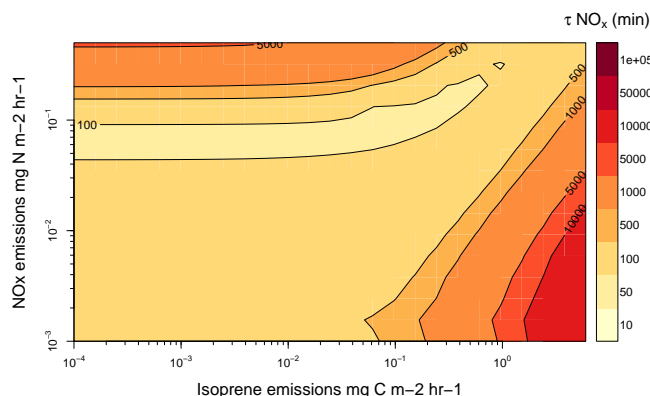

Figure 2. τNO_x (min) isopleth plot as a function of NO_x and isoprene emissions for the Master Chemical Mechanism (MCMv3.2). This was created from a series of box model runs.

nisms we investigated in UKCA using a simple box model. The simulations we performed were aimed at understanding how mechanistic assumptions affected the simulation of O_3 by comparing the results of the reduced mechanisms to the MCM.

As discussed in Sect. 1, the inherent assumptions regarding mechanism reduction (Jeffries et al., 1992), and specifically the omission of unique isoprene oxidation products, may lead to large discrepancies for simulated O_3 between the mechanisms. Here we hypothesise that assumptions about the sequestration of HO_x (via organic hydroperoxides ROOH) and NO_x (via organic nitrates $RONO_2$) are a key cause of inter-mechanism variability and lead to changes in the abundance and hence lifetime of NO_x.

To test this hypothesis, for each mechanism, box model runs were performed at a series of different NO_x and isoprene emission rates, so that an O_3 isopleth plot could be constructed, similar to those found in Dodge (1977) and Sillman and He (2002). In general, all mechanisms produce the same overall behaviour of increasing O_3 with increasing isoprene and NO_x emissions. These general features can be seen
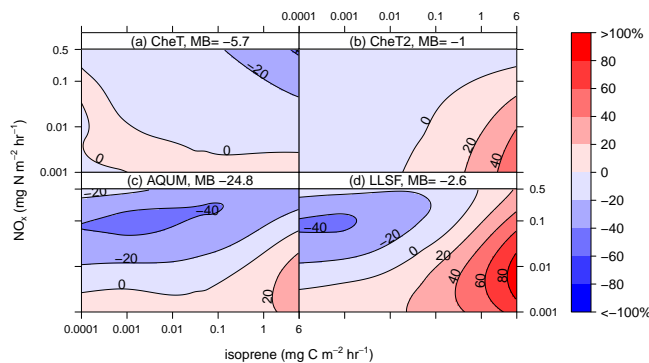

Figure 3. O_3 (percentage difference from the MCM, Fig. 1) isopleth plot as a function of NO_x and isoprene emissions for different isoprene chemical mechanisms. Also quoted for each plot is the mean bias (MB) from the MCM.

in Fig. 1 for the MCM. When both NO_x and isoprene are low, O_3 stays around the initial concentration (30 ppb). As emission rates of both O_3 precursors increase, O_3 increases reaching a maximum of 140–160 ppb at the highest emission rates used (0.5 mg N m^{-2} h^{-1} of NO_x and 6 mg C m^{-2} h^{-1} of isoprene – top right-hand corner). When isoprene emissions are low and NO_x emissions are high (top left-hand corner) net O_3 destruction occurs that is consistent with high nitric acid formation (O_x loss via $NO_2 + OH$). When isoprene emissions are high and NO_x emissions are low, as in a tropical rainforest, (lower right-hand corner) net O_3 destruction occurs as is consistent with high levels isoprene ozonolysis and loss of O_3 via reactions with HO_x. Considering that the box model in some cases does not reach equilibrium, the precise numbers reported here (e.g. 140–160 ppb) are not of significance to the real world where removal processes (i.e. deposition of intermediate compounds and O_3 and NO_x) exist. The overall behaviour of O_3 in Fig. 1 is shown to be related to the overall behaviour of the NO_x lifetime (Fig. 2), defined using Equation 1 from Browne and Cohen (2012). Fig. 2 shows that the NO_x lifetime varies by over 2 orders of magnitude over the range of NO_x and isoprene emissions the simulations covered. A general feature of Fig. 2 is that the NO_x lifetime shows a degree of anticorrelation with the O_3 mixing ratios simulated. Regions of the O_3 isopleth where net O_3 destruction occurs coincide with regions where the NO_x lifetime is greatest. The key cause of this is a reduction in the abundance of OH.

Our main focus is on the comparison of the reduced mechanisms with the MCM for the simulated O_3 mixing ratios and NO_x lifetimes. Figures 3 and 4 show the differences in the O_3 and NO_x lifetimes simulated using the reduced mechanisms relative to the MCM. These differences provide us with useful information about variations in chemical oxidation between the schemes, which may be used to help diagnose the impact of isoprene mechanism differences in the more complex context of the global model experiments (Sect. 4).

3.1 LLSF

LLSF is the most simplistic scheme with no unique species used to represent the chemistry of isoprene, beyond those used to describe the oxidation of methane. Thus, there is only a small amount of NO_x locked up in methyl nitrate formation (reflecting the small yield of methyl nitrate production) and HO_x is efficiently sequestered into organic hydroperoxides (reflecting the slow rates of reactivity of methyl hydroperoxide). Figure 3d shows that using LLSF results in the highest biases in O_3 compared to the MCM of all the mechanisms considered. Under low-NO_x high-isoprene emissions, LLSF is biased high by up to ~ 80 %. Because the reaction between MeO_2 and HO_2 is slower than for the major isoprene-derived peroxy radicals in the MCM, mixing ratios of peroxy radicals are found to be higher in this region, and the enhanced rate of $RO_2 + NO$ leads to high O_3. This is consistent with the differences in the NO_x lifetime (Fig. 4d) which show that under these conditions, the LLSF mechanism simulates an overall shorter NO_x lifetime. This shorter lifetime is reflected across most of the VOC : NO_x emission space with the exception of high-NO_x emissions, where there is better agreement with the MCM (biases ~ 10 %). A band of low-bias in O_3 (Fig. 3d) is correlated with a band of high-bias in NO_x lifetime (Fig. 4d) under a range of low isoprene emissions and moderately high NO_x emissions. Both of these features are consistent with the parameterised instantaneous loss of two OH for the isoprene + OH reaction in LLSF. With LLSF, the low bias at low isoprene emissions and high bias at high isoprene emissions largely cancel each other out, leading to a small overall MB (-2.6 %) for O_3 with respect to the MCM (Fig. 3d). Despite a small overall bias, the majority of the regions where isoprene chemistry is known to be important for the O_3 budget are the regions where this mechanism shows greatest bias.

3.2 AQUM

As discussed in Sec. 2.1, AQUM was developed for representing the oxidation of isoprene in the context of simulating regional air quality. As such AQUM does not account for the formation of organic nitrates, other than from the reaction of isoprene with NO_3. Under low-NO_x high-isoprene emissions, AQUM is biased high by ~ 20 % (Fig. 3c). The figure shows that there is a band of large negative MB (-25 %) in O_3, compared to the MCM, under NO_x emissions of 0.01–0.1 mg N m^{-2} h^{-1}. There is very little correlation between the biases in O_3 and biases in the NO_x lifetime (Fig. 4c) under these emissions. In regions of high-isoprene high-NO_x emissions AQUM simulates much greater values of NO_x lifetime than the MCM, consistent with a reduction in the abundance of NO_x (Browne and Cohen, 2012) and a reduction in OH. Whilst the reduction in the abundance of NO_x, as evidenced by the increase in NO_x lifetime, is consistent with a reduction in the potential for producing O_3, it cannot be as-
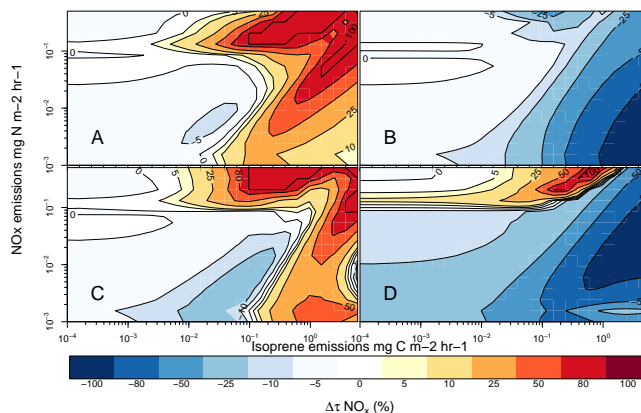

Figure 4. τNO_x (percentage difference from the MCM, Fig. 2) isopleth plot as a function of NO_x and isoprene emissions for different isoprene chemical mechanisms: (A) CheT, (B) CheT2, (C) AQUM, (D) LLSF.

cribed to sequestration of NO_x in organic nitrates and the attribution of the origin of this behaviour lies beyond the scope of this investigation.

3.3 CheT

CheT, which is based on the MIM (Pöschl et al., 2000) was developed for global-scale modelling studies of atmospheric chemistry. As with AQUM, it accounts for the formation of isoprene nitrates produced via NO_3 chemistry but also includes the generation of isoprene nitrates from the OH initiated oxidation (the primary route for isoprene oxidation). Fig. 3a shows the bias in O_3 simulated using CheT compared with the MCM. The bias in O_3 is generally within ± 20 % of the MCM over all the emissions of isoprene and NO_x we investigated. Under high-NO_x and high-isoprene emissions, the bias is higher, with CheT simulating up to 40 % less O_3 than the MCM. Under these conditions CheT also simulates an increase of the NO_x lifetime, consistent with a reduction in the abundance of NO_x (Fig. 4a). Overall the mean bias (MB) is -5.7 %, indicating a weak negative bias compared to the MCM. This result is consistent with the work of Archibald et al. (2010b) who showed that the CheT scheme (UKCA in their runs) simulated lower levels of O_3 than the MCMv3.1.

3.4 CheT2

The last reduced mechanism that was tested in the box model was CheT2. CheT2 is based on CheT but includes recent updates to the oxidation of isoprene including the formation of IEPOX (Paulot et al., 2009) and modifications to the treatment of isoprene nitrates, allowing regeneration of NO_x and formation of multigeneration nitrates. Figure 3b shows that the low bias in O_3 simulated at high O_3 precursor emissions is much less pronounced in CheT2 than in CheT, being
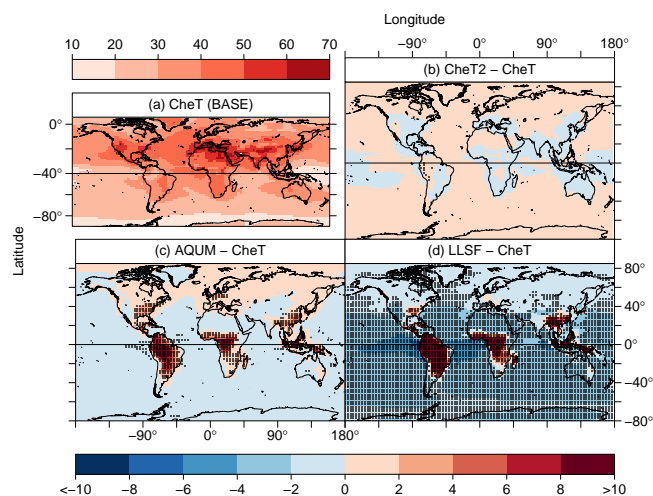
Figure 5. Difference in the present-day (2000, BASE) 5-year mean near-surface ($< 720\,\mathrm{m}$) O_3 (ppb) between CheT isoprene chemistry and other isoprene chemical mechanisms. The stippling indicates where the difference is significant at the 5 % level (greater than $\pm 2.5 \times$ the standard error).

within $\pm 20\,\%$ of the MCM. This is consistent with the lower rate of MPAN formation in CheT2 compared to CheT, meaning that more NO_x is available for O_3 formation. This is also observed in the comparison of the NO_x lifetime. Figure 4b highlights that there is overall a shorter NO_x lifetime (reduction of 50 %) across the range of isoprene and NO_x emissions simulated. Under high-isoprene low-NO_x conditions, the effect of the addition of the ISO_2 HO_x regeneration pathways present in CheT2 (the Peeters mechanism, Peeters et al., 2009) is seen. These were not included in the MCMv3.2, and they serve to enhance HO_x, and decrease NO_x, similar to LLSF. This finding is consistent with the enhanced O_3 seen in Archibald et al. (2011) when CheT (UKCA in their work) was run with inclusion of the Peeters mechanism. Overall the MB of CheT2 with respect to the MCM is lower ($-1\,\%$) than for CheT ($-5.7\,\%$).

3.5   Summary of box model results

These box modelling results show that biases in simulated O_3 are related to the treatments of organic nitrate and organic hydroperoxide chemistry, and to the simulated abundance of NO_x (and its lifetime). The box modelling allows us to examine the effect of the complexity of the chemical processes included and we have shown that we are able to begin to understand the effects of mechanistic differences. It is clear that conclusions drawn solely on the basis of e.g. NO_x lifetime are necessarily incomplete, e.g. in the case of the AQUM biases, and that a detailed analysis of individual reaction fluxes is required to quantitatively understand the origin of biases over the range of emissions used in global model simulations. However, we emphasise that we have not

attempted to perform a systematic study on the isoprene oxidation mechanism. A more rigorous approach would be to examine the individual effects of omissions of mechanistic pathways through one-at-a-time sensitivity tests using one base mechanism, for example the MCM. This is far beyond the scope of our study, which aims to qualify the role of uncertainty in the chemistry vs. the uncertainty in forcings (e.g. emissions) as drivers for the uncertainty of global simulations of O_3. Rather, we aim to link the results from the box model simulations with the global model results (Sect. 4) to provide insight into the behaviour of the isoprene–NO_x–O_3 system. In the following section we will discuss the results of simulations with a global chemistry–climate model where each of the reduced mechanisms is used to assess the impact of using different chemical mechanisms on simulations of climate, land use and emission changes.

4   Present-day mechanism intercomparison with a global model

Using the four reduced schemes, global simulations of the present-day atmosphere were conducted. Figure 5a shows near-surface O_3 for the present day using the CheT isoprene scheme. Figure 5b–d illustrates the change in this O_3 caused by the use of different isoprene chemical schemes. All schemes simulate a present-day tropospheric O_3 burden that is within 1 standard deviation of the model ensemble mean from the ACCENT study (344 ± 39 Tg) (Stevenson et al., 2006). As may be expected from a comparison of isoprene chemical mechanisms, the largest differences between the schemes occur where isoprene emissions are highest (tropical regions and the southeast USA). In these regions (mean isoprene emissions $> 0.1\,\mathrm{mg\,C\,m^{-2}\,h^{-1}}$), the mean surface O_3 for CheT is 41 ppb, whilst for AQUM and LLSF the values are higher – 46 ppb ($+11\,\%$) and 50 ppb ($+18\,\%$) respectively. In some places (e.g. Amazonia, Central Africa), this equates to surface O_3 that is at least 10 ppb higher than with CheT. By comparison, surface O_3 in CheT2 is very similar to that of CheT, even in the high isoprene emitting regions.

The regions of high isoprene emissions, where the largest differences between the mechanisms are calculated, are generally situated away from areas of intense anthropogenic activity. As a result, these areas tend to have low NO_x emissions. To understand the changes occurring in this low-NO_x high-isoprene regime, Table 3 gives the mean O_x budget fluxes for near-surface (below 720 m) grid cells with monthly mean NO_x emissions less than $0.03\,\mathrm{mg\,N\,m^{-2}\,h^{-1}}$ and monthly mean isoprene emissions greater than $0.1\,\mathrm{mg\,C\,m^{-2}\,h^{-1}}$ (roughly matching the bottom right-hand quarter of Fig. 1). Here we define O_x as $O^3P + O^1D + O_3 + 2 \times NO_3 + NO_2 + 3 \times$ dinitrogen pentoxide (N_2O_5) + nitric acid (HNO_3) + peroxynitric acid (HNO_4) + PAN + peroxypropionyl nitrate (PPAN) + MPAN. Figure 6 shows geographical loca-

Table 3. Near-surface (below 720 m) mean O_x budget fluxes (mol gc^{-1} s^{-1}) for regions with high isoprene emissions (greater than 0.1 mg C m^{-2} h^{-1}) and low NO_x emissions (less than 0.03 mg N m^{-2} h^{-1}). Values from the BASE run are given. Also given are the differences caused by climate change (CC) and land use change (LC). See Fig. 6 for which grid cells were used to calculate the values in this table. $\Sigma RO_2 = HO_2 + MeO_2 + RO_2$.

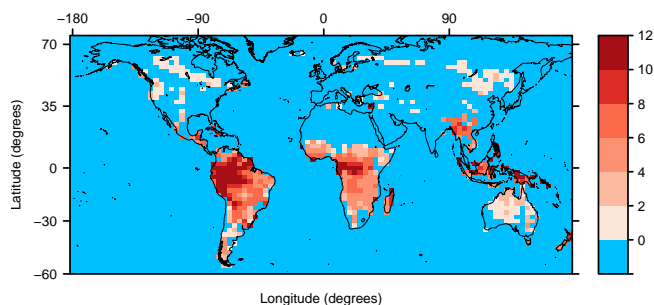| Flux	CheT			CheT2			AQUM			LLSF		
	BASE	CC	LC	BASE	CC	LC	BASE	CC	LC	BASE	CC	LC
$HO_2 + NO$	31	+4.6	+3.3	32	+4.4	+3.2	55	+7.8	−2.2	97	−1.8	−16
$MeO_2 + NO$	12	+2.1	+1.6	11.5	+2.0	+1.8	21	+3.5	−0.2	100	−3.2	−30
$RO_2 + NO$	31	+3.4	−7.0	29	+2.9	−6.7	51	+4.0	−14	2.0	+0.1	+0.7
$OH + RCOOH$	0.0	0.0	0.0	0.0	0.0	0.0	0.0	0.1	0.0	0.1	0.0	0.0
$RONO_2 + OH$	0.3	+0.1	+0.1	0.3	+0.1	0.0	1.4	+0.2	−0.3	0.0	0.0	0.0
$RONO_2 + h\nu$	0.1	0.0	0.0	0.4	0.0	−0.1	0.0	0.0	0.0	0.0	0.0	0.0
$O^1D + H_2O$	29	+2.6	+1.3	29	+2.4	+1.1	35	+3.4	−0.7	43	+1.9	−4.2
Minor loss rxns	0.0	0.0	0.0	0.0	0.0	0.0	0.0	0.0	0.0	0.0	0.0	0.0
$HO_2 + O_3$	8.2	+0.8	−0.1	9.0	+0.8	−0.2	13	+1.6	−1.3	19	−0.3	−4.5
$OH + O_3$	1.4	+0.2	+0.9	1.5	+0.2	+0.9	2.3	+0.5	+0.9	2.8	+0.2	+0.9
O_3 + alkene	20	−2.6	−11	19	−2.7	−10	19	−3.0	−11	18	−3.4	−12
$N_2O_5 + H_2O$	0.0	0.0	0.0	0.0	0.0	0.0	0.0	0.0	0.0	0.2	0.0	0.0
NO_3 Loss	2.9	+0.5	−0.2	3.0	+0.5	−0.3	4.7	+0.5	−1.1	3.8	0.0	−1.1
NO_y Wet Dep	0.7	0.0	+0.2	0.7	0.0	+0.2	0.9	+0.1	+0.2	1.4	−0.1	−1.1
$\Sigma RO_2 + NO$	74	+10	−2.1	73	+9.3	−1.5	130	+15	−16	199	−4.9	−45
Tot. Chem Prod	74	+10	−2.0	74	+9.4	−1.7	130	+16	−17	200	−4.9	−45
Tot. Chem Loss	62	+1.6	−8.7	62	+1.3	−8.4	75	+3.0	−13	89	−1.6	−20
Net Chem	13	+8.6	+6.7	12	+8.0	+6.7	53	+13	−4.0	110	−3.2	−24
O_3 Dry Dep	330	+14	+2.4	330	+12	−0.2	390	+18	−23	490	−6.1	−74
NO_y Dry Dep	10	0.0	−0.1	10	+0.1	0.0	11	+0.1	−0.1	9.9	+0.7	+0.2

Figure 6. Grid cells included in the calculation of the mean O_x budget fluxes reported in Table 3. Units range from 0 to 12, indicating the number of months per year that each grid cell was included in the calculation. Using emissions from the BASE run, only those months when mean isoprene emissions were greater than 0.1 mg C m^{-2} h^{-1} and mean NO_x emissions were less than 0.03 mg N m^{-2} h^{-1} were included. Blue indicates that, based on this criterion, the grid cell was not included in the calculation at all.
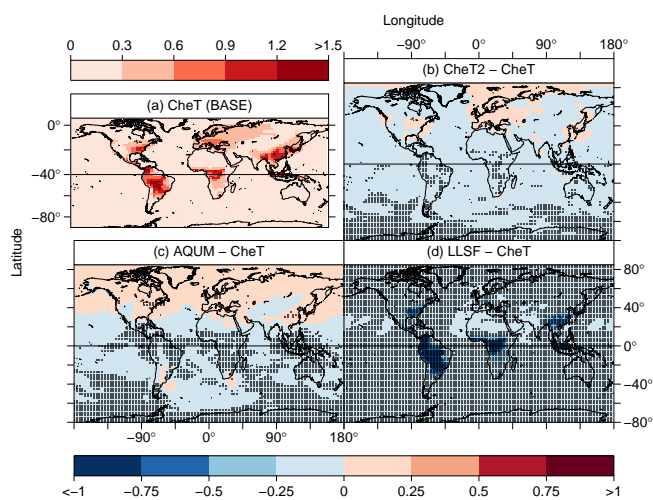
tions of those grid cells included in this emissions regime, and also indicates how many months per year each grid cell was included.

From the budget terms in Table 3 for the BASE integrations, total mean O_x production varies across the schemes from 74 mol gc^{-1} s^{-1} (here gc is grid cell) (CheT and CheT2) to 200 mol gc^{-1} s^{-1} (LLSF). The majority of this variance is due to differences in the peroxy-radical + NO reactions ($HO_2 + NO$, $MeO_2 + NO$ and other peroxy-radicals (RO_2) + NO). In CheT, CheT2 and AQUM, RO_2 is primarily ISO_2, $MACRO_2$ (see Table 1 for definitions) and the peroxy acetyl radical ($MeCO_3$).

In all schemes, the oxidation of isoprene by OH is a source of peroxy radicals. In CheT, CheT2 and AQUM, the initial isoprene + OH reaction leads exclusively to the production of ISO_2, whilst for LLSF MeO_2 is produced instead. Both MeO_2 and ISO_2 may react with NO producing O_x (propagation), or with other peroxy radicals producing peroxides (termination). $k_{ISO_2+HO_2}$ (similar in all schemes that include ISO_2) is three times higher than $k_{MeO_2+HO_2}$ (identical in all schemes), and k_{MeO_2+NO} (identical in all schemes) is two times higher than k_{ISO_2+NO} (similar in all schemes that include ISO_2). This suggests that the scheme that produces the largest fraction of MeO_2 from isoprene oxidation (LLSF) should also show the highest total $RO_2 + NO$ flux and consequently highest O_3 levels, exactly as calculated (see Fig. 5d).

Table 4. Whole tropospheric O_x budget (Tg yr^{-1}) and O_3 burden (Tg) in the BASE run for different mechanisms, and changes due to climate change (CC), isoprene emissions with climate change (IC), anthropogenic emissions (AC), and land use (LC).

Experiment	Mechanism	Prod	Loss	Net Chem	Influx	Dry Dep	Burden (Tg)
BASE	CheT	6188	5706	482	−673	1155	379
	CheT2	6234	5742	492	−662	1154	380
	AQUM	6234	5776	458	−733	1191	374
	LLSF	5979	5480	499	−681	1180	360
CC	CheT	361	540	−179	−165	−14	380
	CheT2	349	530	−181	−165	−16	380
	AQUM	350	515	−165	−149	−17	374
	LLSF	329	500	−171	−150	−21	360
IC	CheT	90	75	15	7	8	383
	CheT2	113	94	20	9	11	385
	AQUM	128	97	31	17	14	380
	LLSF	154	122	32	11	21	367
AC	CheT	−196	−131	−65	−30	−35	379
	CheT2	−160	−112	−47	−12	−36	380
	AQUM	−188	−109	−80	−44	−36	376
	LLSF	−160	−109	−51	−23	−28	364
LC	CheT	−294	−297	3	39	−36	361
	CheT2	−314	−317	3	41	−38	361
	AQUM	−351	−350	−1	49	−50	357
	LLSF	−346	−305	−41	22	−63	346

Figure 7. Difference in the present-day (2000, BASE) 5-year mean near-surface (< 720 m) ΣPAN (ppb) between CheT isoprene chemistry and other isoprene chemical mechanisms. The stippling indicates where the difference is significant at the 5 % level (greater than $\pm 2.5 \times$ the standard error).

In CheT, CheT2 and AQUM, once ISO_2 is formed, it may be further oxidised to produce second-generation peroxy radicals such as $MACRO_2$. In AQUM, reactions of ISO_2 and $MACRO_2$ with NO lead to greater production of O_3, as evident from the higher mean $RO_2 + NO$ flux (Table 3): 51 (AQUM), 31 (CheT), 29 mol gc^{-1} s^{-1} (CheT2). The reason for this is the inclusion in CheT and CheT2 of competing peroxy radical + NO reaction channels that do not lead to O_3 formation. AQUM does not include the isoprene nitrate formation pathway from ISO_2, which accounts for 4.4 and 10 % of the total ISO_2 + NO flux in CheT and CheT2 respectively (Jenkin, 2012). Additionally, AQUM does not include MPAN formation from $MACRO_2 + NO$, which contributes to a lower mean $MACRO_2 + NO \rightarrow NO_2$ flux in CheT and CheT2 compared to AQUM: 7.0 (CheT), 6.7 (CheT2) and 12 mol gc^{-1} s^{-1} (AQUM).

Figure 7 shows total peroxyacyl nitrates (ΣPAN = PAN + MPAN + PPAN) near the surface in (a) CheT and (b–d) the difference between CheT and the other schemes. Figure 7d shows that, compared to CheT, there is much less ΣPAN in LLSF (the ΣPAN tropospheric burden in LLSF is 1.49 Tg compared to 3.57 Tg in CheT). This follows since in LLSF, no ΣPAN precursor radicals ($MeCO_3$ nor $MACRO_2$) are produced from isoprene oxidation. As PANs are a source of O_x to remote regions, the low ΣPAN in LLSF is likely the cause of the low O_3 compared to CheT over the remote tropical oceans (a mean reduction of 10 % between $\pm 20°$ lat., Fig. 5d). Another consequence of reduced PAN formation is that more NO_x stays close to the isoprene source region.
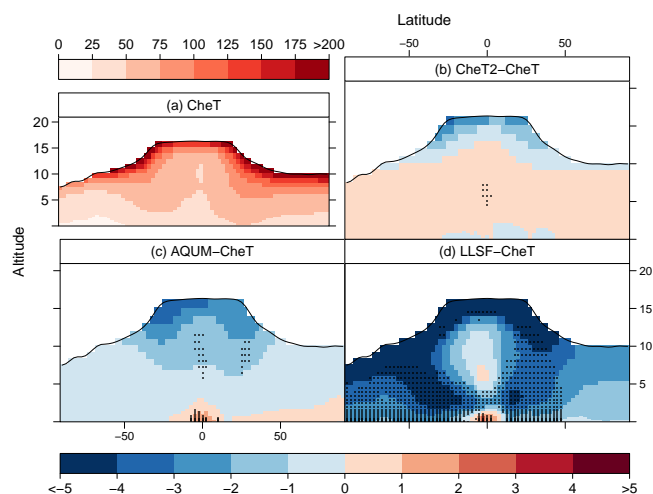
Figure 8. Difference in the present day (2000, BASE) five year mean zonal O_3 (ppb) between CheT isoprene chemistry and other isoprene chemical mechanisms. The stippling indicates where the difference is significant at the 5 % level (greater than $\pm 2.5 \times$ the standard error).

Figure 9. Difference in the present-day (2000, BASE) 5-year mean O_3 dry deposition rate $(\text{mol gc}^{-1}\,\text{s}^{-1})$ between CheT isoprene chemistry and other isoprene chemical mechanisms. The stippling indicates where the difference is significant at the 5 % level (greater than $\pm 2.5 \times$ the standard error).

This contributes to the higher total $RO_2 + NO$ flux, and hence higher O_3, in these regions in LLSF.

Figure 7b indicates that ΣPAN in CheT2 is marginally lower than in CheT (the ΣPAN tropospheric burden is about 6 % lower). The cause of this is that the MPAN production rate in CheT2 is set to be 10 % of that in CheT. The CheT2 rate is the value we would recommend, as it has been adjusted to take account of the fact that in UKCA, the species $MACRO_2$ represents a set of peroxy radicals, not just the MPAN precursor methacrolyl peroxy radical (Jenkin, 2012).

Figure 7c shows that ΣPAN in AQUM is again marginally lower than in CheT (tropospheric ΣPAN burden is 7 % lower), this time due to the total absence of MPAN formation. However, the difference is small owing to the fact that in AQUM PAN production is faster, a result of higher production of the PAN precursor radical $MeCO_3$ from isoprene oxidation. The mean mixing ratio of $MeCO_3$ is 29 % higher than the average of that in CheT and CheT2. Possible additional sources of $MeCO_3$ in AQUM are the higher yield of methyglyoxal (MGLY), which rapidly reacts to form $MeCO_3$ (CheT and CheT2 = 16 Tg MGLY yr^{-1}, AQUM = 40 Tg MGLY yr^{-1}). The higher yield of the $MeCO_3$ peroxy radical also accounts for a fraction of the higher $RO_2 + NO$ flux, and hence higher O_3 in AQUM.

Extending the comparison to the wider troposphere, Table 4 gives the summed total O_x budget fluxes for the different schemes up to the tropopause. Fig. 8 shows the zonal mean ozone for the entire troposphere. The tropopause is shown by the black line. It is immediately apparent that the differences in O_3 at the surface are not representative of the net effect on O_3 over the entire troposphere. Whilst the O_3 burdens of CheT and CheT2 are very similar (379 and
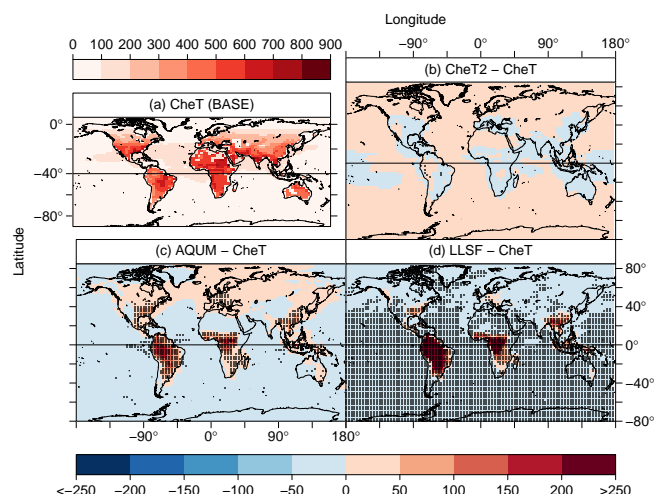
380 Tg, respectively), AQUM has a lower burden (374 Tg) and LLSF lower still (360 Tg). This is consistent with the zonal difference plots (Fig. 8b–d), which show that away from the surface, both AQUM and LLSF give lower O_3 than CheT, most notably in the tropical tropopause region.

Although the highest total tropospheric net chemical O_3 production rate is calculated for LLSF, (499 Tg yr^{-1}), overall the O_3 burden is lower due to the higher rate of dry deposition (1180 Tg yr^{-1}) compared to CheT (1155 Tg yr^{-1}) and CheT2 (1154 Tg yr^{-1}) (see Fig. 9). The rate of dry deposition in AQUM is also high (1191 Tg yr^{-1}) (Fig. 9c). In UM-UKCA dry deposition only occurs at the surface and is highest over forested regions. As AQUM and LLSF both produce higher O_3 near the surface and notably over forested regions (high isoprene emitting regions), dry deposition is likely to be higher. This is indeed the case as illustrated by Fig. 9, which shows much higher O_3 dry deposition fluxes over forested regions (e.g. Amazonia, central Africa) in AQUM and LLSF compared to CheT. CheT and CheT2 have higher rates of ΣPAN formation, leading to more O_3 production away from forested regions and the surface in general, thus resulting in lower O_3 dry deposition and higher overall tropospheric O_3 burdens.

Although tropospheric O_3 varies little between CheT and CheT2 (Figs. 5 and 8), there are larger changes in other key oxidants, notably OH. Due to the inclusion of additional HO_x regeneration pathways within the isoprene oxidation mechanism of CheT2 (namely the Peeters mechanism, Peeters et al., 2009), one would expect CheT2 to show higher levels of OH over high isoprene emitting regions. Figure 10 shows that OH in CheT2 is indeed higher than in CheT over the main isoprene emitting regions, with maximum increases
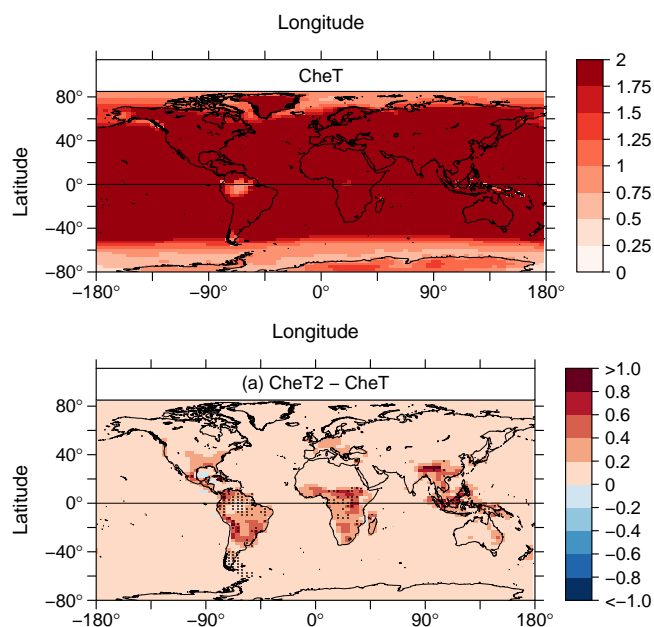
Figure 10. BASE 5-year mean near-surface (below 720 m) OH (10^6 molecule cm^{-3}) in **(a)** CheT and **(b)** the difference between CheT and CheT2. The stippling indicates where the difference is significant at the 5 % level (greater than $\pm 2.5 \times$ the standard error).

Figure 11. Changes in 5-year mean near-surface (< 720 m) O$_3$ (ppb) (2095–2000) caused by climate change (CC) for different isoprene chemical mechanisms. The stippling indicates where the difference is significant at the 5 % level (greater than $\pm 2.5 \times$ the standard error).

of approximately 50 %. Warwick et al. (2013) also calculated that including the Peeters mechanism in UM-UKCA gave higher OH, improving agreement between modelled and measured values.

Levels of the main night-time oxidant, NO$_3$, are higher in CheT2, AQUM and LLSF than in CheT (not shown). By percentage, the largest increases are calculated in the main isoprene emitting regions (Tropics). Here CheT2 shows increases in NO$_3$ compared to CheT of around 30 %, whereas AQUM and LLSF show much greater increases in NO$_3$ – up to 7 times more. This is a consequence of the lower formation rates of nitrate reservoirs in these schemes – thus NO$_3$ formed from the base non-isoprene chemistry, by reactions such as N$_2$O$_5$ photolysis, is removed more slowly. These differences in NO$_3$ levels have implications for the simulated rate of oxidation at night. As key oxidants, differences in both OH and NO$_3$ are important for secondary organic aerosol (SOA) formation, which requires the formation of oxidised organic products.

Another mechanistic difference between CheT2 and CheT that has the potential to affect SOA production is the inclusion of epoxide formation in CheT2, based on the work of Paulot et al. (2009). In the tropics high levels of epoxides (50–70 ppt) reach an altitude of nearly 5 km, and similar mixing ratios are present even in the lower Tropical Tropopause Layer (TTL) (10–13 km). Isoprene-derived epoxides are known to be precursors of organic aerosol formation (Paulot et al., 2009; Surratt et al., 2010), and as such, the presence of epoxides at high tropical altitudes could have
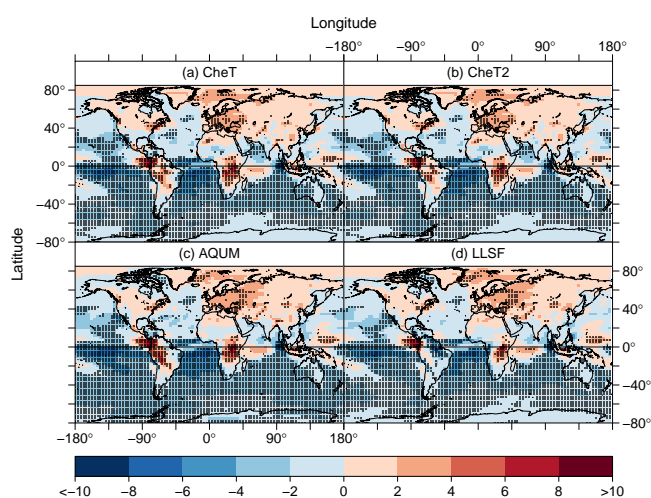
important implications for cloud formation (e.g. Froyd et al., 2010).

5 Future perturbation experiments

In the previous section, we compared the different isoprene mechanisms under present-day conditions. In this section we examine how the mechanisms compare in the context of the future climate change (Sect. 5.1) and future isoprene emission change (Sect. 5.2) perturbation experiments described in Sect. 2.2.2.

5.1 Climate change

Figure 11a shows the change in near-surface O$_3$ caused by our climate change scenario (CC) using the CheT scheme, as in Squire et al. (2014). Figure 11b–d shows the effect of CC using the CheT2, AQUM and LLSF isoprene schemes respectively. The general pattern of near-surface O$_3$ changes is similar in all schemes. There are reductions over the oceans due to increased water vapour and subsequent loss of O$_3$ via increased O^{1}D + H$_2$O. Over land where O$_3$ production dominates (e.g. polluted Northern Hemispheric regions), near-surface O$_3$ increases as the flux through O$_x$ producing reactions usually increases with temperature. In regions with high isoprene emissions such as the Tropics, O$_3$ also tends to increase, due to changes in PAN. PAN decomposition exhibits a strong temperature dependence, such that under the higher temperatures of climate change PAN decomposes faster, thus more NO$_x$ will be present near the isoprene emission source. As a result, the mean ΣRO$_2$ ($=$ HO$_2$ + MeO$_2$ + RO$_2$) + NO flux increases in these re-
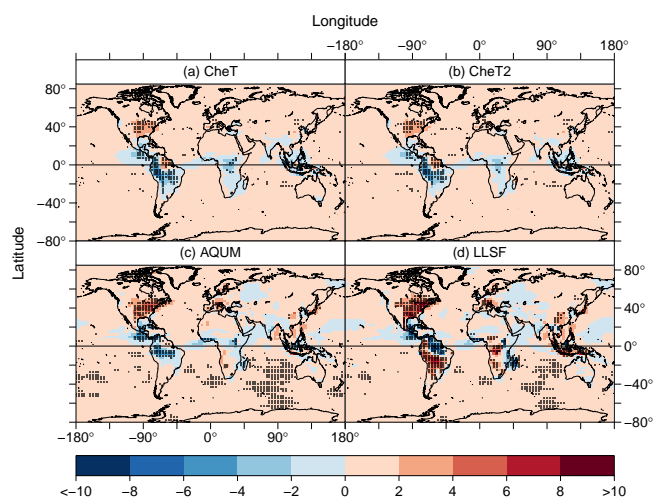
Figure 12. Changes in 5-year mean near-surface ($< 720\,\mathrm{m}$) O_3 (ppb) (2095–2000) caused by the change in isoprene emissions with climate (IC) for different isoprene chemical mechanisms. The stippling indicates where the difference is significant at the 5 % level (greater than $\pm 2.5 \times$ the standard error).

Figure 13. Changes in 5-year mean near-surface ($< 720\,\mathrm{m}$) O_3 (ppb) (2095–2000) caused by land use change (LC) for different isoprene chemical mechanisms. The stippling indicates where the difference is significant at the 5 % level (greater than $\pm 2.5 \times$ the standard error).

gions (see CC entries in Table 3) (AQUM $= +15$, CheT $= +10$, CheT2 $= +9.3\,\mathrm{mol\,gc^{-1}\,s^{-1}}$), leading to higher O_3 near the isoprene emission source.

Unlike with the other schemes, O_3 decreases in high-isoprene low-NO_x regions in simulations using LLSF. This is because LLSF produces very little PAN compared to the other schemes (see Sect. 4), so no increase in NO_x with temperature is calculated as would occur with increased PAN decomposition. The fact that O_3 actually decreases is due to the negative temperature dependence of $k_{C_5H_8+OH}$. The flux through this reaction under climate change decreases by $\sim 20\,\%$ in all schemes, leading to associated increases in OH and isoprene export. Lower isoprene oxidation rates lead to a lower rate of peroxy radical production, and thus the $HO_2 + NO$ and $MeO_2 + NO$ reaction fluxes decrease in LLSF (-1.8 and $-3.2\,\mathrm{mol\,gc^{-1}\,s^{-1}}$, respectively, Table 3). In schemes other than LLSF, this effect is masked by the large increase in NO_x from increased PAN decomposition. Despite large changes in tropospheric net chemical production due to climate change, the tropospheric O_3 burdens in the CC experiment remain unaltered (Table 3).

We also explored how ozone changes with our future anthropogenic emission scenario (AC, not shown). This scenario is characterised by large reductions in NO_x emissions over the USA, Europe and Japan. The O_3 response was remarkably similar for all the different isoprene mechanisms, presumably because the largest changes in anthropogenic emissions occur away from regions of high isoprene emissions. We conclude that the O_3–NO_x response in these regions is controlled largely by the simple NO_x–HO_x chemistry which is the same in all chemistry schemes. If, instead, the scenario had included large NO_x changes in the
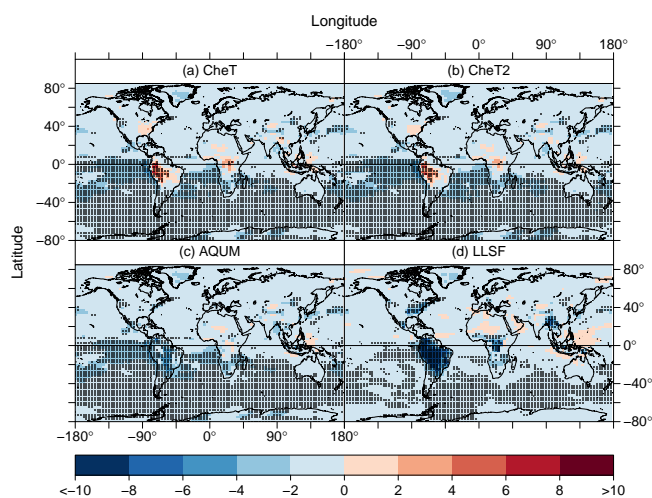
Tropics where isoprene emissions are high, it is likely that the schemes would respond differently. It has previously been shown that changes in tropical NO_x associated with increased anthropogenic activity can lead to large changes in O_3, e.g. Paulot et al. (2012) found that tropical O_3 increased by 30 % when NO_x emissions everywhere were set to those of the USA in terms of GDP per capita. Conducting a similar experiment with different isoprene chemical mechanisms would be a worthwhile extension to our work.

5.2 Isoprene emission change

In this section, we examine the results of the two isoprene emission change experiments: IC (the change in isoprene emissions with climate) and LC (the change in isoprene emissions with land use).

Figures 12 and 13 show the changes in surface O_3 that occur for each of the different isoprene chemical mechanisms in the IC and LC experiments respectively. In both cases, the isoprene mechanism sensitivity is more pronounced than for the CC experiment (Sect. 5.1), which may be anticipated given that the perturbations in IC and LC specifically involve isoprene. On the scale of the whole troposphere, the O_3 burden is enhanced in IC and reduced in LC for all schemes (Table 4). This is expected as in IC, ultimately, there is more O_3 precursor and in LC there is less.

In the next three sections, we analyse the O_3 trends in Figs. 12 and 13 using the corresponding O_x budget terms in Tables. 3 and 5. This is done for each distinct O_x production regime; Sect. 5.2.2 – NO_x-limited regions where isoprene emissions increase, Sect. 5.2.3 – NO_x-limited regions where isoprene emissions decrease, and Sect. 5.2.4 – VOC-limited

regions where isoprene emissions increase. In the next section (Sect. 5.2.1), we discuss how each of these regimes is defined.

5.2.1 Defining distinct O_x production regimes

In the IC experiment, a mean global increase in isoprene emissions ($+78\,\mathrm{Tg\,C\,yr^{-1}}$) is calculated. Within the high isoprene emitting regions, there are three distinct regimes of change, which we will denote as IC regions 1, 2 and 3 (ICr1, ICr2 and ICr3). Each regime is defined on a per-month-per-grid-cell basis as follows:

1. ICr1 is months when isoprene emissions in a grid-cell increase by more than 0.05 Tg and the environment is NO_x-limited.

2. ICr2 is months when isoprene emissions in a grid-cell decrease by more than 0.05 Tg and the environment is NO_x-limited.

3. ICr3 is months when isoprene emissions in a grid-cell increase by more than 0.005 Tg and the environment is VOC-limited.

The isoprene emission change criteria is an order of magnitude smaller for ICr3 than for ICr1 or ICr2, owing to the greater sensitivity of increasing isoprene emissions in a VOC-limited environment compared to a NO_x-limited environment. Here we define VOC-limited as where the ratio of L_N (loss of radicals from reactions with NO and NO_2) to Q (the sum of all radical sinks) is more than 0.5 (Kleinman et al., 1997; Wiedinmyer et al., 2006). NO_x-limited is defined as where L_N/Q is less than 0.5 (Kleinman et al., 1997; Wiedinmyer et al., 2006). To ensure that each regime includes the same grid cells in CheT, CheT2, AQUM and LLSF, L_N/Q values from CheT were used in all cases. The geographical location of those grid cells included in each regime are shown Fig. 14, indicating also how many months per year each grid cell was included. Table 5 gives mean O_x budget fluxes for these three regimes, which will be discussed in Sects. 5.2.2–5.2.4.

In LC, the pattern of change in all high isoprene emitting regions is the same as that of ICr2: reductions in isoprene emissions ($-190\,\mathrm{Tg\,C\,yr^{-1}}$ globally) in a NO_x-limited environment. As such, LC and ICr2 will be discussed together. Note that those high isoprene-emitting regions that were VOC-limited in IC (ICr3, e.g. southeastern USA) are NO_x-limited in LC owing to the inclusion of an anthropogenic emission scenario of large Northern Hemispheric NO_x emission reductions. The mean O_x budget terms for LC are given in Table 3. These were calculated using the same grid cells as the other budgets in this table (see Fig. 6).
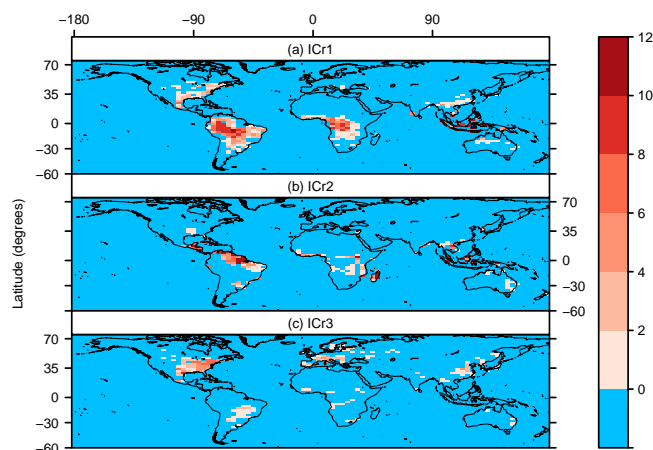

Figure 14. Grid cells included in the calculation of the mean O_x budget fluxes reported in Table 5. Units range from 0 to 12, indicating the number of months per year that each grid cell was included in the calculation. For each region (ICr1, ICr2 and ICr3) different criteria were used to select which months a grid cell should be included, as follows: **(a)** ICr1 is months when isoprene emissions increase by more than 0.05 Tg and the environment is NO_x-limited. **(b)** ICr2 is months when isoprene emissions decrease by more than 0.05 Tg and the environment is NO_x-limited. **(c)** ICr3 is months when isoprene emissions increase by more than 0.005 Tg and the environment is VOC-limited. See text for how NO_x-limited and VOC-limited are defined. Blue indicates that, according to the above criteria, the grid cell was not included in the calculation at all.

5.2.2 NO_x-limited regions where isoprene emissions increase (ICr1)

In ICr1 (where isoprene emissions increase in a NO_x-limited environment), both total chemical O_x production and total chemical O_x loss increase in all schemes, owing to greater O_3 precursor emissions. Changes in O_x loss are similar in all schemes, being driven largely by an increase in isoprene ozonolysis (in the range $+21$ to $+27\,\mathrm{mol\,gc^{-1}\,s^{-1}}$ across the schemes). On the other hand, total O_x production varies considerably between schemes, from $\sim +1\,\mathrm{mol\,gc^{-1}\,s^{-1}}$ in CheT and CheT2, to $+90\,\mathrm{mol\,gc^{-1}\,s^{-1}}$ in LLSF. The overall result is a decrease in net O_x production for CheT and CheT2 (each $-16\,\mathrm{mol\,gc^{-1}\,s^{-1}}$), close to no net change in AQUM, and a net increase in LLSF ($+50\,\mathrm{mol\,gc^{-1}\,s^{-1}}$). As explained in Sect. 4, the primary peroxy radical produced from isoprene oxidation in LLSF is MeO_2, whilst in the other schemes it is ISO_2 and $MACRO_2$. MeO_2 has a higher propensity for reaction with NO than ISO_2 or $MACRO_2$, thus an increase in isoprene emissions (as in ICr1) will increase the total $RO_2 + NO$ flux by a greater amount in LLSF than in the other schemes. Note that the MPAN and isoprene nitrate formation pathways that compete directly with O_x production from isoprene-derived peroxy radicals in CheT and CheT2 are not included in AQUM. Accordingly, increasing

Table 5. Changes in the near-surface (below 720 m) mean O_x budget fluxes from the IC experiment (mol gc^{-1} s^{-1}). The budget is split into three regimes; ICr1 – NO_x-limited regions with large increases in isoprene emissions, ICr2 – NO_x-limited regions with large decreases in isoprene emissions, and ICr3 – VOC-limited regions with large increases in isoprene emissions. See Fig. 14 for which grid cells were included in each regime, and see text for precise definitions of the regimes.

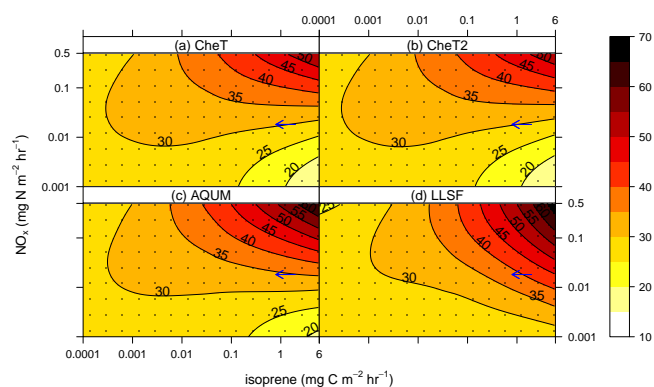| Flux	CheT			CheT2			AQUM			LLSF		
	ICr1	ICr2	ICr3	ICr1	ICr2	ICr3	ICr1	ICr2	ICr3	ICr1	ICr2	ICr3
$HO_2 + NO$	−6	+14	+14	−6	+14	+15	+2	−17	+27	+33	−60	+29
$MeO_2 + NO$	−3	+9	+1	−3	+9	+1	−1	−3	+5	+58	−93	+27
$RO_2 + NO$	+11	−35	+15	+10	−33	+15	+23	−59	+23	−1.4	+3.7	−0.9
$OH + RCOOH$	0	0	−0.2	0	0	−0.1	0	0	−0.1	0	0	−0.1
$RONO_2 + OH$	−0.1	−0.4	+0.5	−0.1	−0.2	+0.2	−0.0	+0.0	−0.0	−0.0	+0.0	−0.0
$RONO_2 + h\nu$	+0.0	−0.0	+0.0	+0.0	−0.4	+0.1	−0.0	−0.0	+0.0	+0.0	−0.0	+0.0
$O^1D + H_2O$	−3	0	+0.9	−3	+1	+0.9	−1	−4	+1.7	+6	−12	+2.0
Minor loss rxns	0	0	0	0	0	0	0	0	0	0	0	0
$HO_2 + O_3$	0	0	+1.3	0	−1	+2.1	0	−6	+4.0	+7	−10	+2.6
$OH + O_3$	−2	+5	−0.8	−2	+5	−0.7	−2	+4	−0.1	−2	+3	−0.2
$O_3 + alkene$	+22	−16	+1.9	+21	−14	+1.6	+24	−15	+1.9	+27	−13	+1.7
$N_2O_5 + H_2O$	0	0	−0.3	0	0	−0.3	0	0	−0.3	0	0	+0.0
NO_3 Loss	0	−3	+3.2	0	−3	+2.9	+2	−5	+2.9	+2	−4	+1.9
NO_y Wet Dep	0	0	−0.5	0	0	−0.4	0	0	−0.3	0	0	−0.0
$\Sigma RO_2 + NO$	+2	−12	+30	+1	−10	+31	+24	−79	+55	+90	−149	+55
Tot. Chem Prod	+1.9	−12	+31	+0.7	−9.8	+32	+24	−79	+56	+90	−149	+54
Tot. Chem Loss	+17	−13	+5.7	+16	−11	+6.2	+23	−26	+9.8	+40	−36	+7.9
Net Chem	−16	−0.4	+25	−16	+1.4	+26	+1.1	−53	+46	+50	−113	+47
O_3 Dry Dep	−25	0	+35	−23	+3	+34	−12	−33	+58	+51	−81	+66
NO_y Dry Dep	−1	+6	−1.4	−1	+6	−0.8	−1	+3	+2.4	−1	+2	+0.4

Figure 15. Monthly mean surface O_3 (ppb) as a function of monthly mean NO_x and isoprene emissions from UM-UKCA. Data from all of the UM-UKCA experiments in this study are used to generate this plot. The NO_x and isoprene emission rates used are identical to those used in Figs. 1 and 3.

isoprene emissions in AQUM leads to a larger increase in the $\Sigma RO_2 + NO$ flux than in CheT or CheT2.

5.2.3 NO_x-limited regions where isoprene emissions decrease (LC and ICr2)

In LC and ICr2 (where isoprene emissions are reduced in a NO_x-limited environment), the opposite trend is calculated compared to ICr1. Both O_x loss and production decrease due to lower levels of O_3 precursor emissions. As with ICr1, the change in O_x loss is similar in all schemes, being driven by reductions in isoprene ozonolysis (on average −11 (LC) and −15 mol gc^{-1} s^{-1} (ICr2) ($\sim$ −50 %)). On the other hand, total O_x production varies considerably between schemes (from −1.7 (LC) and $\sim$ −10 mol gc^{-1} s^{-1} (ICr2) in CheT and CheT2, to −45 (LC) and −149 mol gc^{-1} s^{-1} (ICr2) in LLSF). The reduction in isoprene emissions causes a proportionally larger decrease in $\Sigma RO_2 + NO$ for LLSF compared to the other schemes due to the preferential formation of MeO_2 from isoprene oxidation compared to other peroxy radicals. This leads to a large reduction in net O_x formation in LLSF (−24 (LC), −113 mol gc^{-1} s^{-1} (ICr2)). For AQUM, the lower rate of formation of NO_x reservoir species compared to CheT or CheT2 leads to a greater reduction in $\Sigma RO_2 + NO$, overall leading to a moderate reduction in net O_x production (−4.0 (LC), −53 mol gc^{-1} s^{-1} (ICr2)). Finally, for CheT and CheT2, the increase in O_3

caused by the reduction in isoprene ozonolysis outweighs reductions in O_3 caused by reductions in $\Sigma RO_2 + NO$, leading overall to increases in net O_x production (each +6.7 (LC), +1.4 mol gc^{-1} s^{-1} (ICr2, CheT2)) or close to no change (-0.4 mol gc^{-1} s^{-1} (ICr2, CheT)).

5.2.4 VOC-limited regions where isoprene emissions increase (ICr3)

For ICr3, where isoprene emissions increase in a VOC-limited environment, all schemes show the same trend of increased near-surface O_3. In such an environment, the effect of adding isoprene favours O_3 production to a far greater extent than O_3 loss, owing to the availability of NO_x. The result is that in all schemes, even CheT and CheT2 that have a lower overall propensity for O_x production, net O_x production increases (+25 (CheT), +26 (CheT2), +46 (AQUM), +47 mol gc^{-1} s^{-1} (LLSF), Table 5).

6 A comparison of O_3 sensitivity to precursor emissions in global and box models

Figure 15 shows O_3 isopleths as a function of NO_x and isoprene emission, similar to that in Fig. 1, but for the reduced schemes and, in this case, using O_3 mixing ratio data from the global UM-UKCA simulations. Data from all of the experiments discussed in Sect. 5 were included in Fig. 15 to maximise the NO_x–isoprene emission space that was covered (the exact same emission values were earlier used to produce Figs. 1 and 3). The arrows in Fig. 15 indicate the mean emission of NO_x and isoprene in the Amazon region, before and after land use change (i.e. those emissions used in the AC and LC integrations). For CheT and CheT2, the gradient of the contours is such that O_3 increases with the isoprene emission change, but for the other two schemes, O_3 decreases. This is consistent with the picture presented in Fig. 13.

Comparing Fig. 15 to Figs. 1 and 3, the principal features of the isopleths derived from the global model are captured well by the box model simulations. This includes resolution of the differences between the schemes, such as the higher O_3 in LLSF and AQUM at high isoprene emissions compared to CheT and CheT2. In fact, compared to the global model, the box model simulations tend to accentuate the chemical differences between the schemes. With the isopleths derived from the global model simulations, the effects of advection and deposition somewhat buffer the chemical differences, leading to a narrower range of O_3 mixing ratios and more similar isopleths. Consequently, the O_3 levels reached in the global simulations (less than 70 ppb) are generally lower than in the box model (approaching 170 ppb). The qualitative agreement between the isopleths derived from the box model and global model suggests that the method of constructing such isopleths with the far less computationally expensive

box models is a convenient way to quickly and accurately assess differences between chemical mechanisms. The fact that Figs. 1, 3 and 15 show good agreement, gives us confidence that use of the box model to compare to a near-explicit mechanism (the MCM) with reduced schemes is relevant for global model experiments.

7 Conclusions

Here we have examined the effect on tropospheric O_3 of using different reduced isoprene chemical mechanisms currently used in ESMs, to simulate the impact of climate change (CC), isoprene emission changes with climate (IC), anthropogenic emission changes (AC), and land use change (LC). Between the CheT and CheT2 schemes, there is no significant difference in near-surface O_3, though OH is higher in isoprene-emitting regions in CheT2 due to the inclusion of additional HO_x regeneration pathways from isoprene oxidation. For the BASE run, in the major isoprene emitting regions AQUM and LLSF give O_3 levels that are at least 10 ppb higher than with the other schemes. This is due to differences in the speciation of peroxy radicals produced by the schemes. LLSF produces a large yield of MeO_2 that rapidly reacts with NO to form O_3. The other schemes produce ISO_2, which has a higher rate of radical termination than MeO_2, thus leading to less O_3 formation. AQUM produces more O_3 than CheT and CheT2 because the scheme makes less ISON and no MPAN – both important NO_x sinks near the isoprene emission source.

Turning to the future perturbation experiments, in CC, the O_3 climate change sensitivity is similar in all schemes, though LLSF responds differently over the Amazon, due to the fact that no PANs are produced. In the anthropogenic emission change experiment (AC) (characterised by large NO_x emission reductions in the Northern Hemisphere), all mechanisms respond in a similar way. This suggests that the O_3–NO_x response is driven largely by the simple NO_x–HO_x–alkane chemistry, which is the same for all schemes.

With the isoprene emission change experiments (IC and LC), there are changes in both isoprene ozonolysis (O_x loss) and the $\Sigma RO_2 + NO$ flux (O_x production). For the land use change experiment (LC), isoprene emissions decrease leading to a reduction in both processes. The ozonolysis changes are the same in all schemes, but the $RO_2 + NO$ reductions differ widely between schemes. For LLSF, reductions are largest owing to the high yield of MeO_2, which favours reaction with NO compared to higher isoprene-derived peroxy radicals (ISO_2 and $MACRO_2$). These are produced by the other schemes, leading overall to a smaller reduction in $RO_2 + NO$. In LLSF and AQUM the reduction in $RO_2 + NO$ is sufficient to cause a net decrease in near surface O_3 in response to land use. This is not the case for CheT and CheT2, however, due to the formation of MPAN and ad-

ditional ISON. For IC (increase in emissions), the opposite trends are calculated, though AQUM is in closer agreement with CheT and CheT2. This is most likely due to smaller net isoprene emission changes in IC compared to LC. In IC (where isoprene emissions increase under VOC-limited conditions (e.g. southeast USA)), all schemes show a net increase in near surface O_3 owing to an increase in isoprene emissions that favours O_x production under such conditions.

Using the CheT scheme, Squire et al. (2014) found that the calculated increases in O_3 due to cropland expansion (LC) were too small to cause a significant increase in O_3-induced vegetation damage. As the three additional mechanisms examined here simulate similar or negative changes in O_3 with cropland expansion, this conclusion would not change with the use of these schemes, and further calculations (not shown) demonstrate this to be the case.

Using the emissions and O_3 data from all of the global model experiments, we were able to construct O_3 isopleths in terms of NO_x and isoprene emissions. These isopleths explain the global model response to isoprene emission changes. Using these same O_3 precursor emissions, we constructed O_3 isopleths using a box model. We find there is good qualitative agreement between those isopleths derived from the global model and those from the box model. This suggests that comparing chemical mechanisms within a box model is a computationally efficient and useful tool for assessing mechanistic performance in complex global models. Furthermore, the agreement between box and global models gives us confidence that the comparison between a box model and a near-explicit mechanism is relevant to the global model experiments. The findings reported here should help to guide mechanistic development strategies. For example, we find that the LLSF scheme produces much higher O_3 near isoprene source regions than the other three schemes. This was the only scheme where only simple peroxy radicals were produced, and, crucially there was no PAN production from isoprene chemistry. Adding simple parameterisation of PAN formation would improve the distribution of O_3. Here, we have shown that the magnitude and even the sign of the O_3 response is affected by the choice of reduced isoprene mechanism.

Edited by: P. O. Wennberg

References

Archibald, A. T., Cooke, M. C., Utembe, S. R., Shallcross, D. E., Derwent, R. G., and Jenkin, M. E.: Impacts of mechanistic changes on HO$_x$ formation and recycling in the oxidation of isoprene, Atmos. Chem. Phys., 10, 8097–8118, doi:10.5194/acp-10-8097-2010, 2010a.

Archibald, A. T., Jenkin, M. E., and Shallcross, D. E.: An isoprene mechanism intercomparison, Atmos. Environ., 44, 5356–5364, doi:10.1016/j.atmosenv.2009.09.016, 2010b.

Archibald, A. T., Levine, J. G., Abraham, N. L., Cooke, M. C., Edwards, P. M., Heard, D. E., Jenkin, M. E., Karunaharan, A., Pike, R. C., Monks, P. S., Shallcross, D. E., Telford, P. J., Whalley, L. K., and Pyle, J. A.: Impacts of HO$_x$ regeneration and recycling in the oxidation of isoprene: consequences for the composition of past, present and future atmospheres, Geophys. Res. Lett., 38, L05804, doi:10.1029/2010GL046520, 2011.

Aumont, B., Szopa, S., and Madronich, S.: Modelling the evolution of organic carbon during its gas-phase tropospheric oxidation: development of an explicit model based on a self generating approach, Atmos. Chem. Phys., 5, 2497–2517, doi:10.5194/acp-5-2497-2005, 2005.

Browne, E. C. and Cohen, R. C.: Effects of biogenic nitrate chemistry on the NO$_x$ lifetime in remote continental regions, Atmos. Chem. Phys., 12, 11917–11932, doi:10.5194/acp-12-11917-2012, 2012.

Cameron-Smith, P., Prather, M. J., Lamarque, J., Hess, P. G., Connell, P. S., Bergmann, D. J., and Vitt, F. M.: The super-fast chemistry mechanism for IPCC AR5 simulations with CCSM, in: American Geophysical Union, Fall Meeting, 18 December 2009, San Francisco, A54A-08, 2009.

Chameides, W., Lindsay, R., Richardson, J., and Kiang, C.: The role of biogenic hydrocarbons in urban photochemical smog – Atlanta as a case-study, Science, 241, 1473–1475, 1988.

Dodge, M.: Combined use of modeling techniques and smog chamber data to derive ozone-precursor relationships, in: Proceedings of the International Conference on Photochemical Oxidant Pollution and its Control, US Environmental Protection Agency, Research Triangle Park, NC, USA, 881–889, 1977.

Farmer, D. K. and Cohen, R. C.: Observations of HNO$_3$, ΣAN, ΣPN and NO$_2$ fluxes: evidence for rapid HO$_x$ chemistry within a pine forest canopy, Atmos. Chem. Phys., 8, 3899–3917, doi:10.5194/acp-8-3899-2008, 2008.

Fiore, A. M., Naik, V., Spracklen, D. V., Steiner, A., Unger, N., Prather, M., Bergmann, D., Cameron-Smith, P. J., Cionni, I., Collins, W. J., Dalsoren, S., Eyring, V., Folberth, G. A., Ginoux, P., Horowitz, L. W., Josse, B., Lamarque, J.-F., MacKenzie, I. A., Nagashima, T., O'Connor, F. M., Righi, M., Rumbold, S. T., Shindell, D. T., Skeie, R. B., Sudo, K., Szopa, S., Takemura, T., and Zeng, G.: Global air quality and climate, Chem. Soc. Rev., 41, 6663–6683, 2012.

Froyd, K. D., Murphy, S. M., Murphy, D. M., de Gouw, J. A., Eddingsaas, N. C., and Wennberg, P. O.: Contribution of isoprene-derived organosulfates to free tropospheric aerosol mass, Proc. Natl. Acad. Sci. USA, 107, 21360–21365, 2010.

Fuchs, H., Bohn, B., Hofzumahaus, A., Holland, F., Lu, K. D., Nehr, S., Rohrer, F., and Wahner, A.: Detection of HO$_2$ by laser-induced fluorescence: calibration and interferences from RO$_2$ radicals, Atmos. Meas. Tech., 4, 1209–1225, doi:10.5194/amt-4-1209-2011, 2011.

Fuchs, H., Hofzumahaus, A., Rohrer, F., Bohn, B., Brauers, T., Dorn, H.-P., Haeseler, R., Holland, F., Kaminski, M., Li, X., Lu, K., Nehr, S., Tillmann, R., Wegener, R., and Wahner, A.: Experimental evidence for efficient hydroxyl radical regeneration in isoprene oxidation, Nat. Geosci., 6, 1023–1026, 2013.

Ganzeveld, L., Bouwman, L., Stehfest, E., van Vuuren, D. P., Eickhout, B., and Lelieveld, J.: Impact of future land use and land cover changes on atmospheric chemistry–climate interactions, J. Geophys. Res., 115, D23301, doi:10.1029/2010JD014041, 2010.

Guenther, A., Karl, T., Harley, P., Wiedinmyer, C., Palmer, P. I., and Geron, C.: Estimates of global terrestrial isoprene emissions using MEGAN (Model of Emissions of Gases and Aerosols from Nature), Atmos. Chem. Phys., 6, 3181–3210, doi:10.5194/acp-6-3181-2006, 2006.

Haagen-Smit, A. J.: Chemistry and physiology of Los Angeles smog, Ind. Eng. Chem. Res., 44, 1342–1346, 1952.

Horowitz, L. W., Fiore, A. M., Milly, G. P., Cohen, R. C., Perring, A., Wooldridge, P. J., Hess, P. G., Emmons, L. K., and Lamarque, J.-F.: Observational constraints on the chemistry of isoprene nitrates over the eastern United States, J. Geophys. Res., 112, D12S08, doi:10.1029/2006JD007747, 2007.

Huntingford, C., Cox, P. M., Mercado, L. M., Sitch, S., Bellouin, N., Boucher, O., and Gedney, N.: Highly contrasting effects of different climate forcing agents on terrestrial ecosystem services, Philos. T. Roy. Soc. A, 369, 2026–2037, 2011.

Jeffries, H. E., Gery, M. W., and Carter, W. P. L.: Protocols for Evaluating Oxidant Mechanisms Used in Urban and Regional Models, Tech. rep., US Environmental Protection Agency, Atmospheric Research and Exposure Assessment Laboratory, Research Triangle Park, NC 27711, 1992.

Jenkin, M.: Review of the atmospheric chemistry of isoprene and evaluation of mechanisms for global modelling, Tech. rep., UK Met Office, Atmospheric Chemistry Services, Oakhampton, Devon, UK, 2012.

Jenkin, M. E., Saunders, S. M., and Pilling, M. J.: The tropospheric degradation of volatile organic compounds: a protocol for mechanism development, Atmos. Environ., 31, 81–104, 1997.

Kleinman, L., Daum, P., Lee, J., Lee, Y., Nunnermacker, L., Springston, S., Newman, L., Weinstein-Lloyd, J., and Sillman, S.: Dependence of ozone production on NO and hydrocarbons in the troposphere, Geophys. Res. Lett., 24, 2299–2302, 1997.

Kubistin, D., Harder, H., Martinez, M., Rudolf, M., Sander, R., Bozem, H., Eerdekens, G., Fischer, H., Gurk, C., Klüpfel, T., Königstedt, R., Parchatka, U., Schiller, C. L., Stickler, A., Taraborrelli, D., Williams, J., and Lelieveld, J.: Hydroxyl radicals in the tropical troposphere over the Suriname rainforest: comparison of measurements with the box model MECCA, Atmos. Chem. Phys., 10, 9705–9728, doi:10.5194/acp-10-9705-2010, 2010.

Kwok, E. S. C. and Atkinson, R.: Estimation of hydroxyl radical reaction-rate constants for gas-phase organic-compounds using a structure-reactivity relationship – an update, Atmos. Environ., 29, 1685–1695, 1995.

Lathiere, J., Hewitt, C. N., and Beerling, D. J.: Sensitivity of isoprene emissions from the terrestrial biosphere to 20th century changes in atmospheric CO_2 concentration, climate, and land use, Glob. Change Biol., 24, GB1004, doi:10.1029/2009GB003548, 2010.

Lee, L., Teng, A. P., Wennberg, P. O., Crounse, J. D., and Cohen, R. C.: On rates and mechanisms of OH and O_3 reactions with isoprene-derived hydroxy nitrates, J. Phys. Chem. A, 118, 1622–1637, 2014.

Lockwood, A. L., Shepson, P. B., Fiddler, M. N., and Alaghmand, M.: Isoprene nitrates: preparation, separation, identification, yields, and atmospheric chemistry, Atmos. Chem. Phys., 10, 6169–6178, doi:10.5194/acp-10-6169-2010, 2010.

Mao, J., Ren, X., Zhang, L., Van Duin, D. M., Cohen, R. C., Park, J.-H., Goldstein, A. H., Paulot, F., Beaver, M. R., Crounse, J. D., Wennberg, P. O., DiGangi, J. P., Henry, S. B., Keutsch, F. N., Park, C., Schade, G. W., Wolfe, G. M., Thornton, J. A., and Brune, W. H.: Insights into hydroxyl measurements and atmospheric oxidation in a California forest, Atmos. Chem. Phys., 12, 8009–8020, doi:10.5194/acp-12-8009-2012, 2012.

McGillen, M. R., Archibald, A. T., Carey, T., Leather, K. E., Shallcross, D. E., Wenger, J. C., and Percival, C. J.: Structure-activity relationship (SAR) for the prediction of gas-phase ozonolysis rate coefficients: an extension towards heteroatomic unsaturated species, Phys. Chem. Chem. Phys., 13, 2842–2849, 2011.

Müller, J.-F., Peeters, J., and Stavrakou, T.: Fast photolysis of carbonyl nitrates from isoprene, Atmos. Chem. Phys., 14, 2497–2508, doi:10.5194/acp-14-2497-2014, 2014.

O'Connor, F. M., Johnson, C. E., Morgenstern, O., Abraham, N. L., Braesicke, P., Dalvi, M., Folberth, G. A., Sanderson, M. G., Telford, P. J., Voulgarakis, A., Young, P. J., Zeng, G., Collins, W. J., and Pyle, J. A.: Evaluation of the new UKCA climate-composition model – Part 2: The Troposphere, Geosci. Model Dev., 7, 41–91, doi:10.5194/gmd-7-41-2014, 2014.

Pacifico, F., Folberth, G. A., Jones, C. D., Harrison, S. P., and Collins, W. J.: Sensitivity of biogenic isoprene emissions to past, present, and future environmental conditions and implications for atmospheric chemistry, J. Geophys. Res., 117, D22302, doi:10.1029/2012JD018276, 2012.

Paulot, F., Crounse, J. D., Kjaergaard, H. G., Kuerten, A., St Clair, J. M., Seinfeld, J. H., and Wennberg, P. O.: Unexpected epoxide formation in the gas-phase photooxidation of isoprene, Science, 325, 730–733, 2009.

Paulot, F., Henze, D. K., and Wennberg, P. O.: Impact of the isoprene photochemical cascade on tropical ozone, Atmos. Chem. Phys., 12, 1307–1325, doi:10.5194/acp-12-1307-2012, 2012.

Peeters, J., Nguyen, T. L., and Vereecken, L.: HO_x radical regeneration in the oxidation of isoprene, Phys. Chem. Chem. Phys., 11, 5935–5939, 2009.

Perring, A. E., Bertram, T. H., Wooldridge, P. J., Fried, A., Heikes, B. G., Dibb, J., Crounse, J. D., Wennberg, P. O., Blake, N. J., Blake, D. R., Brune, W. H., Singh, H. B., and Cohen, R. C.: Airborne observations of total $RONO_2$: new constraints on the yield and lifetime of isoprene nitrates, Atmos. Chem. Phys., 9, 1451–1463, doi:10.5194/acp-9-1451-2009, 2009.

Pöschl, U., von Kuhlmann, R., Poisson, N., and Crutzen, P.: Development and intercomparison of condensed isoprene oxidation mechanisms for global atmospheric modeling, J. Atmos. Chem., 37, 29–52, 2000.

Ren, X., Olson, J. R., Crawford, J. H., Brune, W. H., Mao, J., Long, R. B., Chen, Z., Chen, G., Avery, M. A., Sachse, G. W., Barrick, J. D., Diskin, G. S., Huey, L. G., Fried, A., Cohen, R. C., Heikes, B., Wennberg, P. O., Singh, H. B., Blake, D. R., and Shet-

ter, R. E.: HO$_x$ chemistry during INTEX-A 2004: Observation, model calculation, and comparison with previous studies, J. Geophys. Res., 113, D05310, doi:10.1029/2007JD009166, 2008.

Sanderson, M., Jones, C., Collins, W., Johnson, C., and Derwent, R.: Effect of climate change on isoprene emissions and surface ozone levels, Geophys. Res. Lett., 30, 1936, doi:10.1029/2003GL017642, 2003.

Sandu, A. and Sander, R.: Technical note: Simulating chemical systems in Fortran90 and Matlab with the Kinetic PreProcessor KPP-2.1, Atmos. Chem. Phys., 6, 187–195, doi:10.5194/acp-6-187-2006, 2006.

Savage, N. H., Agnew, P., Davis, L. S., Ordóñez, C., Thorpe, R., Johnson, C. E., O'Connor, F. M., and Dalvi, M.: Air quality modelling using the Met Office Unified Model (AQUM OS24-26): model description and initial evaluation, Geosci. Model Dev., 6, 353–372, doi:10.5194/gmd-6-353-2013, 2013.

Shepson, P. B., Mackay, E., and Muthuramu, K.: Henry's law constants and removal processes for several atmospheric β-hydroxy alkyl nitrates, Environ. Sci. Technol., 30, 3618–3623, 1996.

Sillman, S. and He, D. Y.: Some theoretical results concerning O$_3$-NO$_x$-VOC chemistry and NO$_x$-VOC indicators, J. Geophys. Res., 107, 4659, doi:10.1029/2001JD001123, 2002.

Squire, O. J., Archibald, A. T., Abraham, N. L., Beerling, D. J., Hewitt, C. N., Lathière, J., Pike, R. C., Telford, P. J., and Pyle, J. A.: Influence of future climate and cropland expansion on isoprene emissions and tropospheric ozone, Atmos. Chem. Phys., 14, 1011–1024, doi:10.5194/acp-14-1011-2014, 2014.

Stevenson, D. S., Dentener, F. J., Schultz, M. G., Ellingsen, K., van Noije, T. P. C., Wild, O., Zeng, G., Amann, M., Atherton, C. S., Bell, N., Bergmann, D. J., Bey, I., Butler, T., Cofala, J., Collins, W. J., Derwent, R. G., Doherty, R. M., Drevet, J., Eskes, H. J., Fiore, A. M., Gauss, M., Hauglustaine, D. A., Horowitz, L. W., Isaksen, I. S. A., Krol, M. C., Lamarque, J.-F., Lawrence, M. G., Montanaro, V., Müller, J.-F., Pitari, G., Prather, M. J., Pyle, J. A., Rast, S., Rodriguez, J. M., Sanderson, M. G., Savage, N. H., Shindell, D. T., Strahan, S. E., Sudo, K., and Szopa, S.: Multimodel ensemble simulations of present-day and near-future tropospheric ozone, J. Geophys. Res., 111, D08301, doi:10.1029/2005JD006338, 2006.

Stone, D., Evans, M. J., Edwards, P. M., Commane, R., Ingham, T., Rickard, A. R., Brookes, D. M., Hopkins, J., Leigh, R. J., Lewis, A. C., Monks, P. S., Oram, D., Reeves, C. E., Stewart, D., and Heard, D. E.: Isoprene oxidation mechanisms: measurements and modelling of OH and HO$_2$ over a South-East Asian tropical rainforest during the OP3 field campaign, Atmos. Chem. Phys., 11, 6749–6771, doi:10.5194/acp-11-6749-2011, 2011.

Surratt, J. D., Chan, A. W. H., Eddingsaas, N. C., Chan, M. N., Loza, C. L., Kwan, A. J., Hersey, S. P., Flagan, R. C., Wennberg, P. O., and Seinfeld, J. H.: Reactive intermediates revealed in secondary organic aerosol formation from isoprene, Proc. Natl. Acad. Sci. USA, 107, 6640–6645, 2010.

von Kuhlmann, R., Lawrence, M. G., Pöschl, U., and Crutzen, P. J.: Sensitivities in global scale modeling of isoprene, Atmos. Chem. Phys., 4, 1–17, doi:10.5194/acp-4-1-2004, 2004.

Wang, K. and Shallcross, D.: Modelling terrestrial biogenic isoprene fluxes and their potential impact on global chemical species using a coupled LSM-CTM model, Atmos. Environ., 34, 2909–2925, 2000.

Warwick, N. J., Archibald, A. T., Ashworth, K., Dorsey, J., Edwards, P. M., Heard, D. E., Langford, B., Lee, J., Misztal, P. K., Whalley, L. K., and Pyle, J. A.: A global model study of the impact of land-use change in Borneo on atmospheric composition, Atmos. Chem. Phys., 13, 9183–9194, doi:10.5194/acp-13-9183-2013, 2013.

Whalley, L. K., Edwards, P. M., Furneaux, K. L., Goddard, A., Ingham, T., Evans, M. J., Stone, D., Hopkins, J. R., Jones, C. E., Karunaharan, A., Lee, J. D., Lewis, A. C., Monks, P. S., Moller, S. J., and Heard, D. E.: Quantifying the magnitude of a missing hydroxyl radical source in a tropical rainforest, Atmos. Chem. Phys., 11, 7223–7233, doi:10.5194/acp-11-7223-2011, 2011.

Wiedinmyer, C., Tie, X., Guenther, A., Neilson, R., and Granier, C.: Future changes in biogenic isoprene emissions: how might they affect regional and global atmospheric chemistry?, Earth Interact., 10, 1–19, doi:10.1175/EI174.1, 2006.

Wu, S., Mickley, L. J., Jacob, D. J., Logan, J. A., Yantosca, R. M., and Rind, D.: Why are there large differences between models in global budgets of tropospheric ozone?, J. Geophys. Res., 112, D05302, doi:10.1029/2006JD007801, 2007.

Wu, S., Mickley, L. J., Kaplan, J. O., and Jacob, D. J.: Impacts of changes in land use and land cover on atmospheric chemistry and air quality over the 21st century, Atmos. Chem. Phys., 12, 1597–1609, doi:10.5194/acp-12-1597-2012, 2012.

Xie, Y., Paulot, F., Carter, W. P. L., Nolte, C. G., Luecken, D. J., Hutzell, W. T., Wennberg, P. O., Cohen, R. C., and Pinder, R. W.: Understanding the impact of recent advances in isoprene photooxidation on simulations of regional air quality, Atmos. Chem. Phys., 13, 8439–8455, doi:10.5194/acp-13-8439-2013, 2013.